water

MDPI

Article

Slaughterhouse Wastewater Properties Assessment by Modern and Classic Methods

Ramona Crainic [1,2] and Radu Fechete [2,*]

[1] Faculty of Physics, Doctoral School, Babeş-Bolyai University, 1 Kogălniceanu, 400084 Cluj-Napoca, Romania; ramona.crainic95@gmail.com
[2] Physics and Chemistry Department, Technical University of Cluj-Napoca, Str. Muncii 103-105, 400641 Cluj-Napoca, Romania
* Correspondence: rfechete@phys.utcluj.ro; Tel.: +40-741-770-595

Abstract: Advanced ^{1}H Nuclear Magnetic Resonance (NMR) relaxometry and diffusometry methods and VIS-nearIR spectroscopy combined with pH, electrical conductivity (EC) and totally dissolved solids (TDSSs) measurements were used to assess the properties of wastewater collected from a chicken slaughterhouse in each step of the treatment process (wastewater before treatment, biologically treated wastewater, chemically treated wastewater and discharged wastewater) and from sludge. The ^{1}H NMR Carr–Purcell–Meiboom–Gill (CPMG) and Pulsed-Gradient-Stimulated-Echo (PGSE) decay curves recorded for all samples of wastewater were analyzed by inverse Laplace transform (ILT) to obtain the distributions of transverse relaxation times T_2 and diffusion coefficient D. The VIS-nearIR total absorbance, T_2-values, D-values, pH, EC and TDSS parameters were used for statistical analysis in principal component (PCA). The ^{1}H T_2-distributions measured for the slaughterhouse wastewater lie in two main regions reflecting the number of dissolved solids or the distribution of undissolved solids. The PCA analysis successfully differentiates between polluted and less polluted wastewaters and sludge. The wastewater treatment applied by the slaughterhouse is efficient. The recommended methods for wastewater monitoring are the NMR T_2- and D-distributions and EC, TDSSs and NMR-D diffusion coefficient. Finally, Machine Learning algorithms are used to provide prediction maps of wastewater treatment stage.

Keywords: slaughterhouse wastewater and sludge; ^{1}H NMR relaxometry and diffusometry; VIS-nearIR spectroscopy; pH; EC and TDSSs measurements; PCA (principal component analysis); AI-prediction using machine learning

Citation: Crainic, R.; Fechete, R. Slaughterhouse Wastewater Properties Assessment by Modern and Classic Methods. *Water* **2024**, *16*, 2382. https://doi.org/10.3390/w16172382

Academic Editors: Kai He, Jing Wei, Zhishui Liang and Yuanfeng Qi

Received: 3 July 2024
Revised: 15 August 2024
Accepted: 23 August 2024
Published: 24 August 2024

1. Introduction

Nuclear Magnetic Resonance (NMR) is a powerful analytical tool, extensively used for the characterization of microscopic properties of many classes of materials. However, it is not yet favored in the assessment of wastewater properties, particularly in that collected from slaughterhouses. Classical measurements of wastewater characteristics are mainly based on determining the global physicochemical parameters, such as electrical conductivity (EC), total suspended solids (TSSs), total dissolved solids (TDSSs), apparent color, turbidity, pH, chemical oxygen demand (COD) and ammoniacal nitrogen (NH_3-N) of poultry slaughterhouse wastewater (PSW) [1]. Distilled water has a poor electrical conductivity due to the lack of ions. The presence of electrically charged particles is necessary to support the electrical conduction in solutions. Therefore, measuring high electrical conductivity in wastewater clearly indicates the presence of various types of particles, and thus a certain degree of wastewater pollution [2]. Determining the total suspended solids and the total dissolved solids can indicate the amount of undissolved solid pollutants and that of dissolved pollutants, respectively. The TDSSs and/or the TSSs values are usually proportional to the amounts of these solids in the aqueous sample. Depending on the size and the electrical properties of the particles in the wastewater, liquids can present

certain sensitivity to the incident light. Therefore, an apparent color of wastewater can be associated with the presence of specific pollutants. Otherwise, the overall characterization within the visible range can be carried out by performing turbidity measurements. The presence of dissolved or undissolved pollutants may increase its turbidity and therefore reduce the intensity of light transmitted through wastewater samples [3]. Water is a good solvent for a large range of compounds. Therefore, the measurement of wastewater pH value can indicate the pollution level [4,5]. The amount of organic matter in wastewater samples can be determined by classical methods such as: (i) total organic carbon (TOC), directly indicating the organic matter content; (ii) biochemical oxygen demand (BOD), and (iii) chemical oxygen demand measurements. The last two (BOD and COD) offer an indirect quantification of the total organic matter content in aqueous samples. The biochemical oxygen demand is related to the biodegradable organic content of samples. This can be quantified by measuring the oxygen consumption by microorganisms present in the water samples [6,7]. Another indicator of the total organic content is the presence of ammonia, an inorganic compound that demands and consumes oxygen during the process of conversion to nitrate. Other parameters that may complete characterization of wastewater quality may include: (i) the chemical variables such as, ammonia (NH_3), chloride (Cl^-), nitrates ($NO_3{}^-$), orthophosphates ($-PO_4^{-3}$), sulphates ($SO_4{}^{2-}$), oxidation reduction potential (ORP), total nitrogen (TN) or total phosphorus (TP); (ii) microbiological variables, such as fecal coliforms (FC), total coliforms (TC), or *Escherichia coli* (*E. coli*) [8–10]. Relative recently, Aatik et al. developed a wastewater quality index (WWQI) to estimate the overall quality status of the raw and treated wastewaters. This is a number that can cumulatively describe the quality of an aggregate set of measured physicochemical and biological parameters [10]. For example the (waste)water can be described as: (i) poor for WWQI between 0 and 44; (ii) marginal for WWQI from 45 to 64; (iii) fair for WWQI from 65 to 79; (iv) good for WWQI from 80 to 94, and (v) excellent for WWQI from 95 to 100 [10,11].

Throughout all the stages in the slaughterhouse production line, large amounts of water are consumed (15–20 L/chicken), thus also requiring an intense processing of resulting wastewater. This is loaded with organic matter that may re-enter the environment in large amounts, via effluents [1,12]. It is therefore essential to apply efficient purification treatments of wastewater prior to release. Wastewater management is considered an important task, subjected to strict global regulations [13–15]. Some well-established physicochemical methods, used to treat the wastewater by removing contaminants such as metals, organic matter (OM) and total suspended solids, are [16]: coagulation–flocculation [17,18]; flotation [19,20]; electrocoagulation [21,22]; chemical precipitation [1,17,23–25]; ultra- and nano-membrane filtration and reverse osmosis [26,27]. Traditionally, biological (aerobic and anaerobic) treatment methods have been used for poultry slaughterhouse wastewater treatment. Unfortunately, both biological techniques present some limitations [28]. The conventional treatment processes of agro-industrial wastewater based on the aerobic technologies requires high energy consumption for aeration and generates large amounts of sludge. In recent years, these tend to have been replaced by more environmentally friendly anaerobic biotechnologies. Among others, for the slaughterhouse wastewater treatment, the sequencing batch reactor (SBR) showed a good efficiency for pollutant removal [15,28,29].

Classical measurements of wastewater properties based on determining the electrical conductivity, TSSs, TDSSs, turbidity, pH or COD values are far from an accurate description. Moreover, in many situations, within experimental errors, the samples cannot be differentiated using only these parameters. By comparison with usual situations, anyone can imagine that, knowing only the average age, it is difficult to describe the population structure of a country or, knowing the average wage, it is difficult to guess the distribution of income for the employees of a company. Similarly, knowing just a single value of a parameter, describing globally a complex sample with many components like wastewater, can dramatically limit any improvement in treatment methods. In these situations, improvement very often comes from a strategy of trial and error. Conversely, implementing characterization methods capable of discriminating between different components, and

characterizing them, allows an educated strategy for an efficient improvement of treatment by knowing the mechanism of interaction between the treatment agent and sample (wastewater in this particular case). Such methods are based on Laplace spectroscopy, such as NMR relaxometry and diffusometry, or classical Fourier spectroscopy, such as FT-IR or UV-VIS.

NMR is one of the most widely used characterization methods for a large variety of materials, from plastics to elastomers [30–33], ordered tissues [34,35], denaturation of keratin [36,37], proton exchange membranes [38,39], biomaterials [40], construction materials [41] or even for in vivo human tissues [42]. With the exception of plastic/elastomers, for all other materials ^{1}H NMR implies the study of water states. H_2O is seen as a group of "spy" molecules in interaction with organic and inorganic materials. A logical step was to apply the well-known ^{1}H NMR methods, such as: (i) one-dimensional ^{1}H NMR relaxometry, to obtain the transverse relaxation times T_2-distribution, sensitive to water pools dimension [13,41,43,44]; (ii) one-dimensional ^{1}H NMR diffusometry to obtain the distribution of self-diffusion coefficient D, sensitive to molecular water mobility and water pools restrictions [31]. These two NMR parameters are sensitive to water impurities, and thus different water components can be revealed. For example, in slaughterhouse wastewater can be found: (i) soluble impurities that will increase the wastewater viscosity reducing the T_2 and D values or (ii) insoluble impurities that, depending on their dimensions, can be seen as different relaxation environments leading to multiple T_2-values. Having different sizes and different hydrophilicity (or hydrophobicity), such impurities can act (or not) as transport vehicles for water molecules. Then, one can observe multiple values in the measured D-distribution. The NMR data are analyzed by the inverse Laplace transform (ILT) [45–48]. In this way, one can obtain the distribution of relevant NMR parameters to describe the wastewater states by water components [13,41,43,44,49–52].

The aim of this study is to assess the efficiency of new methods, such as low field ^{1}H NMR relaxometry and diffusometry and VIS-nearIR spectroscopy in analyzing the polluted wastewater (PSW) during the treatment process in the slaughterhouse. The advantage of these methods resides in their ability to offer a large range (distribution) of the measured parameters. The sample apparent color is used to characterize the wastewater contamination with impurities. Such soluble or insoluble impurities can increase the turbidity of wastewater samples. In this study, we aim to better characterize these two parameters by VIS-nearIR spectra measured for a range of wavelengths from 390 to 980 nm. Afterwards, we show how the non-classical methods can be combined with the classical methods which characterize the entire wastewater samples, for a complex analysis using Principal Component (PCA) [53,54]. Thus, PCA statistical data lead to graphic plots that are easily interpreted to discriminate between all types of wastewater (at least between the polluted and less polluted). Thus, the PCA can be used to evaluate the treatment process efficiency and can offer information about the relevance of each measured parameter in the characterization of the PSW purification. Moreover, it can be used in combination with machine learning algorithms to provide predictions related to the stage of the treatment process. In this way, the integrated combination of NMR relaxometry and diffusiometry with VIS-nearIR spectroscopy and conventional measurements, such as pH, EC and TDSS in PCA analysis, enhanced by predictions performed by an ANN machine learning algorithm, will provide a comprehensive assessment of wastewater properties. This integrative approach ensures a thorough evaluation of the treatment process at various stages!

2. Materials and Methods

2.1. Materials and Processes in the Slaughterhouse Wastewater Purification Treatment

The wastewater and sludge samples were collected from a chicken slaughterhouse located in the northwestern part of Romania, from winter to spring in four different months. The main components of chicken slaughterhouse purification treatment plant are presented in Figure 1. The untreated wastewater was collected from the pumping basin where the wastewater is brought directly from the slaughterhouse. This wastewater contains all the

specific organic matter pollutants resulting from the slaughterhouse, such as dejection, fodder, gastric contents, blood, fragments of meat and intestines, fats, feather remnants, etc. From here, the wastewater is pumped by a parabolic filter that allows only the wastewater and small particles to pass, while the large residues are collected by gravitation in an external tank (see Figure 1). Next, the wastewater is stored in a large pool, where it is periodically mixed by aeration to avoid the sedimentation of heavy matter. From here, the wastewater is pumped in a flotation basin for chemical treatment. This treatment is performed in the presence of SUPERFLOC C-2240 (registered trademark) liquid cationic polymer. According to the producers, this liquid coagulant polymer acts as primary coagulant, being a charge neutralization agent in the liquid/solid separation processes. The liquid polymer enables filtration, flotation of dissolved air, wastewater clarification, and reduces the use of inorganic salts. It is used at a ratio of approximately 1.8 L of liquid polymer to 1000 L of wastewater, but the effective dose is pH controlled.

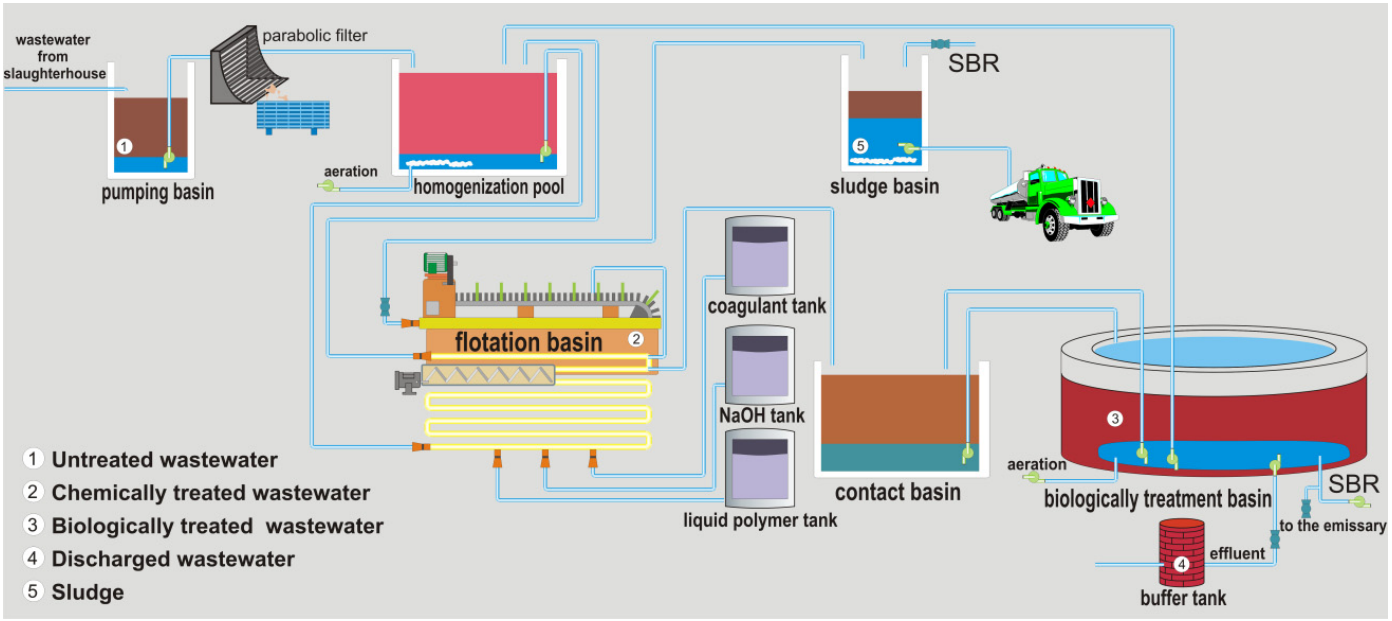

Figure 1. The main components of the wastewater purification treatment plant of a chicken slaughterhouse.

The second chemical agent is sodium hydroxide (NaOH), popularly known as caustic soda (or lye). This is a highly caustic base, used to decompose the proteins remained in the wastewater. Ferric sulphate is the third chemical agent, typically used for wastewater treatment and sludge conditioning, for removing phosphorus, to reduce the hydrogen sulphate, and to attenuate the corrosiveness and odor of wastewater and sludge. Being lighter than water, the coagulated sludge is collected from the wastewater surface in the flotation basin with a paddled conveyer belt and is stored in a sludge basin. From here, it is then transported to another city to be used in producing biogas.

The sludge samples were collected from the sludge basins, as shown in Figure 1. The chemically treated wastewater samples were collected from the bottom of the flotation basin through a drain hole (see Figure 1). After its separation from sludge, the chemically treated wastewater is pumped in the contact tank that communicates with an external basin where the liquid undergoes the biological treatment process. This is mainly based on the anaerobic bacterial treatment in a classical sequencing batch reactor, also shown in Figure 1. In this biological treatment basin, the bacterial population is controlled by wastewater retraction in the contact basin and/or by aeration. The samples of biologically treated wastewater were collected in daylight during the purification process. The bio-purification technology implies numerous steps. To be discharged after a sequence of nitrification, the wastewater is subjected to a 2 h stage of nitro-sedimentation, followed

by another 2 h stage of sedimentation. The control mechanism of the wastewater station only allows the wastewater to be discharged after these 4 h of sedimentation stage, which usually takes place overnight. The samples of discharged, and hence completely treated wastewater, were collected from a buffer tank located between the slaughterhouse treatment plant and the Crasna River flowing nearby. The sediments collected at the bottom of the biological treatment basin are pumped back in the homogenization pool, and re-enter to the purification circuit, again undergoing chemical treatment and separation from sludge in the flotation basin. Thus, the sludge results are combined from both the biological and the chemical treatments.

The wastewater samples (untreated wastewater, chemically treated wastewater, biologically treated wastewater, discharged wastewater) and sludge were each stored each in ½ L plastic containers, immediately transported to the analytical laboratory at the Technical University of Cluj-Napoca (TUCN), and the analyses run as soon as possible (1 to 3 days). Prior to each measurement, the samples were homogenized by manually agitating the bottles for 1–3 min. Between the successive sets of measurements the wastewater samples were stored in the transport bottles at room temperature and protected from light.

2.2. Methods

The first set of measurements were performed for the overall parameters: pH, electrical conductivity and totally dissolved solids. The second set of measurements consisted of the ^{1}H NMR relaxometry that lasted several minutes per measurement. The ^{1}H NMR diffusometry measurements were the longest, lasting approximately 80 min per sample. Finally, the FT-IR spectra (not discussed here) were the last performed measurements, requiring in total 5 min per sample [13].

The ^{1}H NMR relaxometry and diffusometry measurements for all the wastewater samples were performed using a Bruker Minispec MQ 20 (Bruker Co., Ettlingen, Germany) spectrometer working at 19.69 MHz. The NMR relaxation data were recorded using the well-known CPMG (Carr–Purcell–Meiboom–Gill) pulse sequence [13,41,42] with echo time 2τ = 2 ms (Figure S1a, in Supplementary Information). A total of 3000 echoes were registered, and the repetition time or recycle delay (RD) was set at 3 s. For a good signal-to-noise ratio (Figure 2a), acquiring 32 scans was sufficient [13]. Then, the experimental data were processed using a fast inverse Laplace-like transform (ILT) algorithm, increasingly used in recent years to analyze multi-exponential decay curves [13,42,44–46]. The NMR self-diffusion data were recorded using the pulsed gradient stimulated echo (PGSE) pulse sequence (Figure S1b in Supplementary Information). The inter echo time τ was set at 3 ms, the encoding and decoding pulse gradients duration δ was 0.4 ms, while the self-diffusion time Δ was set at 20 ms. A number of 64 acquisitions were collected with a recycle delay of 1.5 s. The recorded data were analyzed by the ILT algorithm with the proper (see below) kernel. The ILT analysis [45–48] will be described in Section 2.3 below.

The Vis-nearIR spectra were recorded in less than 10 s per sample, using a PASCO spectrometer. For some wastewater samples, a sedimentation time was necessary before each measurement. The sludge samples were distilled at a ratio of 1:20, by adding 1 mL sludge to 20 mL of distilled water. The measurement set-up was as follows: (i) the lower wavelength λ_L was 379.928 nm; (ii) the higher wavelength λ_H was 950.11 nm; (iii) a total number of 2132 points were acquired with a resolution of 0.268 nm; (iv) 25 scans were accumulated to increase the signal-to-noise ratio (SNR).

The pH and the electrical conductivity were measured using a water quality meter multi-parameter Model 8603. The totally dissolved solids were measured using a pocket TDSS/EC meter. All the methods of measurement/analysis follow the standard protocols [1].

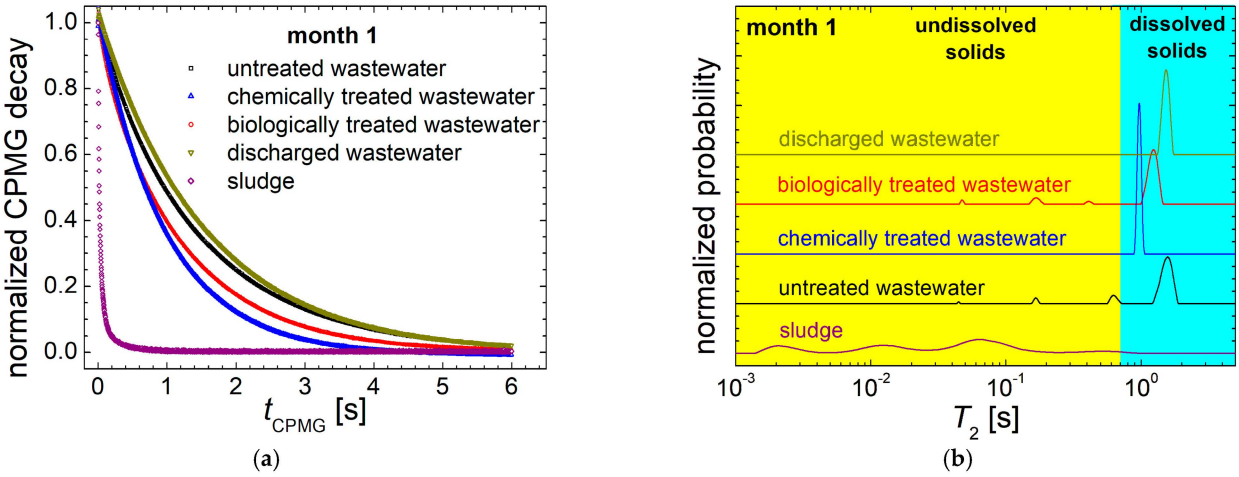

Figure 2. (**a**) The normalized CPMG decays recorded for the slaughterhouse wastewater (untreated–black square, chemically treated–blue upper triangle, biologically treated–red circle and discharged wastewater–dark yellow lower triangle) and sludge (diamonds) collected in month 1 of monitoring; (**b**) the normalized T_2-distributions of the CPMG decay curves presented in (**a**).

2.3. Data Analysis

The CPMG decays of nuclear magnetization, $M(t_{CPMG})$ characteristic of water with many types of impurities (see Figure 2a), are assumed to be multi-exponential. Each specific transverse relaxation time describes a certain spin dynamics according to the ^{1}H environment. Therefore, the $M(t_{CPMG})$ decay can be written as [42–44]:

$$M(t_{CPMG}) = \sum_{i=1}^{N} P(T_{2,i}) exp\left\{-\frac{t_{CPMG}}{T_{2,i}}\right\}, \quad (1)$$

where $P(T_{2,i})$ is the probability of finding a statistical spin ensemble (water ^{1}H) characterized by a specific transverse relaxation time $T_{2,i}$ [36]. $t_{CPMG} = \tau_2 = 2n\tau$ is the total duration of the CPMG experiment, as can be seen from Figure S1a in the Supplementary Information. To consider a real distribution of transverse relaxation times, the decay of the nuclear magnetization presented in Equation (1) can be considered to have an integral Laplace-like form that also contains the distribution function of transverse relaxation times $f(T_2)$ [42–48]:

$$F(t) = \int_0^{+\infty} f(T_2) exp\left\{-\frac{t}{T_2}\right\} dT_2. \quad (2)$$

Nevertheless, the practical way to analyze the discretized acquired NMR signal is to combine the finite summation presented in Equation (1) and the distribution function $f(T_2)$. Finally, the goal of an inverse Laplace analysis is to find a normalized distribution function $f(T_2)$. This will be interpreted as normalized probability to find a statistically relevant number of water ^{1}H characterized by a particular value of T_2. Here, we have to remark that the transverse relaxation process assumes a certain loss of phase of the nuclear spins processing around a static magnetic field, and at the same time being in interaction with neighboring spins. Therefore, for just an isolated spin, the T_2 is not defined.

Similarly, the decay of the normalized pulsed field gradient echo (PGSE) NMR signal can be viewed in an integral Laplace-like form containing the specific distribution function $f(D)$ of the self-diffusion coefficient [41,46]:

$$\frac{S(g)}{S(0)} = \int_0^{+\infty} f(D) \exp\left\{-\gamma^2 g^2 \delta^2 D\left(\Delta - \frac{\delta}{3}\right)\right\} dD = \int_0^{+\infty} f(D) \exp\{-bD\} dD, \quad (3)$$

where D is the self-diffusion coefficient and the distribution function $f(D)$ is the parameter function to be obtained. The new kernel of Laplace-like integral presented in Equation (3) contains the ^{1}H gyromagnetic ratio γ; the magnetic field gradient strength g; the duration of encoding/decoding pulsed gradients δ and the self-diffusion time Δ.

2.4. Statistical Analysis

In general it is not possible to directly compare the behavioral effects of two parameters of different types, though a standard method is largely used to analyze the statistical data (usually from more than one group) that are characterized by numerous variables or observables having different measurement units. This is multivariate analysis, in particular, principal components analysis [54]. For our study, we implemented our own numerical program in MatLab 2020 and we plotted the results in Microsoft Excel software 2024. For such PCA statistical analysis, a data matrix is produced containing the input values that will be discussed later in Table 1. As variables, we selected: (i) the total absorbance from the Vis-nearIR spectra; (ii) the most probable transverse relaxation time $T_{2,1}$ characteristic to wastewater with dissolved solids, from ^{1}H NMR relaxometry measurements; (iii) the most probable self-diffusion coefficient D_1 specific also to wastewater with dissolved solids, from ^{1}H NMR diffusometry measurements; and the bulk values for (iv) pH; (v) electrical conductivity and (vi) totally dissolved solids. All the values of these six parameters were considered for all our five groups of four samples, each of them corresponding to one month of monitoring. The values of these parameters form the input matrix with 6 columns and 20 rows. The results of the PCA method will be largely discussed later in the text.

Table 1. The values of relevant parameters (total VIS-nearIR absorbance, the most probable transverse relaxation time $T_{2,1}$, the self-diffusion coefficient D_1, pH, electrical conductivity EC and the total dissolved solids TDSS) measured for the slaughterhouse wastewater (untreated, chemically treated, biologically treated and discharged) and sludge collected during four months of monitoring.

Wastewater	Month	Total VIS-NearIR Absorbance	$T_{2,1}$ [s]	D_1 [10^{-9} m^2/s]	pH [-]	EC [µS/cm]	TDSS [ppm]
untreated wastewater	1	1.06 *	1.57	2.76	5.11	478	263
	2	0.14	1.71	2.86	6.75	1596	795
	3	1.40 *	1.31	2.78	7.16	1236	618
	4	2.13 *	1.59	2.81	7.17	658	658
chemically treated wastewater	1	0.06	0.96	3.03	8.4	947	470
	2	0.04	1.36	2.88	6.03	860	484
	3	0.05	1.02	2.90	6.35	740	374
	4	0.02	0.89	2.95	6.53	383	383
biologically treated wastewater	1	0.33 **	1.24	2.68	7.15	1182	597
	2	0.14 **	0.58	2.81	7.29	822	412
	3	2.99 **	0.47	2.68	6.25	686	344
	4	0.04 **	0.33	2.67	6.66	353	353
discharged wastewater	1	0.02	1.53	2.98	7.52	860	433
	2	0.02	1.30	2.86	5.84	429	429
	3	0.03	0.99	2.91	6.56	704	352
	4	0.002	1.04	2.88	6.61	356	356
Sludge	1	1.39 ***	0.52	2.31	7.23	2880	1662
	2	0.33 ***	0.32	2.62	6.92	2070	1045
	3	0.43 ***	0.34	2.66	6.13	1668	826
	4	0.32 ***	0.14	2.60	6.94	963	963

Notes: * Measured after 30 min of sedimentation; ** measured after 10 min of sedimentation; *** measured after 5 min of sedimentation; in all cases the measurement errors are smaller than 5%.

2.5. Prediction Using Machine Learning ML5, an AI-Based Algorithm

The two-dimensional PC1-PC2 map obtained from PCA analysis were used for an advanced prediction of probability maps from any newly assumed measurements using the machine learning library ML5 [55,56]. For this, a dedicated program was written in JavaScript following the descriptions presented in [56] and adapted for our purpose. The 20 (=5 × 4) values obtained from PCA analysis was used to train an Artificial Neural Network (ANN) with a learning rate of 10% and for 10,000 epochs. The resulting model was saved and reloaded to predict the probability of a new measurement, located on each element of a 100 × 100 matrix correlated to the PC1-PC2 map obtained from the PCA analysis, associated with each type of wastewater or sludge.

3. Results

3.1. ^{1}H NMR Relaxometry of Wastewater and of Sludge from the Chicken Slaughterhouse

The results obtained by measuring the normalized ^{1}H nuclear magnetization decays during the CPMG pulse sequence for all types of wastewater and sludge samples collected over the first month of monitoring are compared in Figure 2a. At 6 s, a complete decay (less than 5% from initial magnetization) is observed for all the wastewater samples, indicating a large mobility of water molecules. An equivalent decay is observed for sludge (purple diamond in Figure 2a), but this is achieved in less than 0.2 s, indicating, as expected, a strong mobility limitation for the water molecules. Among wastewater samples, the slowest decay was measured in discharged wastewater (dark yellow down triangle), which is expected to present the smallest number of impurities.

Chemically (blue upper triangle) and biologically (red circle) treated wastewaters present the fastest decays, suggesting the presence of large amounts of undissolved solids and/or dissolved solids, and/or the presence of paramagnetic impurities.

A much better analysis of the normalized ^{1}H nuclear magnetization decays, providing deeper information about water state and efficiency of treatment process, can be achieved by an inverse Laplace analysis [42–48]. The normalized transverse relaxation time T_2-distributions obtained from ILT of CPMG decays measured for slaughterhouse wastewater (untreated, chemically and biologically treated and discharged wastewater) and for sludge are presented in Figure 2b. The normalized probability function $f(T_2)$ presents a series of peaks at different T_2–values covering more than three orders of magnitude from 1 ms up to 3 s. From left to right (from small to large T_2–values) these peaks can be associated with water molecules being in different environments. For example, the ^{1}H with more restricted mobility are characterized by small T_2–values, while water ^{1}H with less restricted mobility are characterized by large T_2–values. Considering the specificity of our samples, one can divide the full domain of T_2–values in two main subdomains. Thus, there is the range of T_2–values from 1 ms up to 700 ms, of water molecules attached to undissolved solids (on yellow background), and the subdomain of T_2–values from 700 ms to 3 s (with blue-cyan background) where the particular position of peaks and therefore of the most probable T_2–values is influenced by the type and number of dissolved particles [13]. In particular, we measured for our low filed NMR spectrometer a T_2–value for distilled water (no dissolved or undissolved particles) of 2.66 ± 0.1 s (see Figure 3). The presence of various dissolved solids should be then evaluated by taking into account this reference value. From Figure 2b, for wastewater samples in the subdomain of water pools with dissolved particles, only one peak can be observed, but up to three peaks for water pools with undissolved particles. It is reasonable to assume that the water molecules are attached permanently or can experience a certain exchange between free water and bound water [41] and the attachment is to undissolved particles of different dimensions. The size (and shape, density, and hydrophilicity/hydrophobicity) of such particles can influence the mobility of undissolved particles, hence the mobility of water molecules attached to these particles. The NMR T_2 relaxation time is sensitive to ^{1}H mobility and therefore it is a good parameter to sense and characterize the presence and sizes of such undissolved particles. Furthermore, it is reasonable to assume the fact that large particles will have a small mobility and the

corresponding T_2 relaxation times values are also small. Small particles will have then a large mobility and a large corresponding T_2–value. The integral area under the peaks, as it is measured from the T_2-distributions, is proportional with the number of ^{1}H present in each pool with a specific transverse relaxation time value.

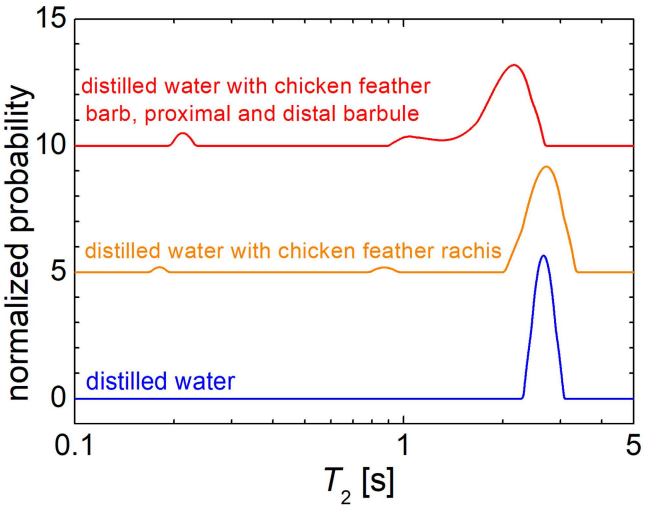

Figure 3. The normalized T_2-distributions recorded for distilled water (bottom blue line), distilled water with chickens feather rachis (middle orange line) and distilled water with chicken feather barb and proximal and distal barbule (top red line).

Considering the above, in Figure 2b it can be observed that the T_2-distributions measured for the untreated wastewater is characterized by four peaks: (i) a large peak (the largest integral area under the peak) in the subdomain of water with dissolved solids with the most probable T_2–value of 1.57 s not so far from the limit of 2.66 s (blue curve in Figure 3), indicating a small number of dissolved solids; (ii) a relatively large peak centered at a T_2–value of ~0.63 s indicating a large number of small undissolved particles; (iii) a relatively medium size peak centered at a T_2–value of ~0.17 s indicating the presence of medium size undissolved particles and (iv) a small (at the observable limit) peak centered at a T_2–value of ~45 ms indicating the presence of relatively large undissolved particles. In general, ^{1}H NMR relaxometry is also a method capable, within certain limits, of offering the size of such particles (or pores [36]), but the experiments need to be performed under more idealistic conditions for inorganic interface water-matter, where a certain surface relaxation parameter has to be estimated, conditions that are not fulfilled in our study. Furthermore, for untreated wastewater, the sampling procedure can play an essential role. For example, in our case, the narrow bore pipette used to insert the sample in the NMR tube was acting as a filter for the larger undissolved fragments that are typically present in untreated wastewater.

The chemically treated wastewater (blue line in Figure 2b) is characterized by a single peak in the subdomains of water with dissolved solids. The fact that no peaks were found in the domain of water with undissolved solids is a good indicator of the efficiency of the coagulation–flotation sludge separation process applied in the chemical treatment basin. On the other hand, the most probable T_2–value of ~0.96 s indicates a larger presence of dissolved solids compared with the T_2–value of ~1.57 s measured for the untreated wastewater. Two processes could explain these findings: (i) the undissolved solids subjected to chemical treatment became soluble in water and (ii) the chemicals (liquid polymer, caustic soda and especially the ferric sulphate) enrich the water with paramagnetic impurities. The measured signal is the narrowest peak, compared to all the peaks measured for wastewater samples, also indicating a high degree of homogeneity of this sample. Surprisingly, the biologically treated wastewater is characterized again by four peaks, one in the subdomain of water with dissolved solids and three in the range of water with

undissolved solids. At first glance this looks like a regression in the treatment process, but one must consider the complex mechanism of wastewater treatment presented in Figure 1. This wastewater sample was collected from the biological treatment basin, in daylight and in the presence of anaerobic bacteria, with nitrification and aeration processes that mixed all components, prior to the nitro-sedimentation and sedimentation. The peaks position in the T_2-distributions measured for the biologically treated wastewater (red distribution function) for water with undissolved solids is almost identical to the position of the peaks obtained for untreated wastewater (black curve). A quality improvement in the water with dissolved solids can be noticed by observing that the most probable T_2–value increases from ~0.96 s (measured for chemically treated wastewater) to ~1.24 s.

The efficiency of the pollutants removal using this sequencing batch reactor for wastewater treatment is observed from the T_2-distributions measured for the discharged wastewater, after several hours allowing for nitro-sedimentation and sedimentation. The T_2-distribution is characterized by a single peak located in the subdomain of water with dissolved solids at a T_2–value of ~1.53 s. The position of this peak is similar to the position of the peak obtained for untreated wastewater sample in the subdomain of water with dissolved solids. Its narrower linewidth indicates less variation in the types of dissolved solids.

The sludge (purple distribution at the bottom of Figure 2b) also presents four peaks, but all of them are characterized by reduced T_2–values, suggesting, as expected, the presence of protons with a reduced mobility. In fact, the term 'water with undissolved solids'; may by inappropriate in this case, since the sludge is a complex colloidal system [44]. Here, a large amount of water is trapped in the organic and inorganic matter, and therefore has a reduced mobility and cannot be easily released. Moreover, taking into consideration the lower limit of T_2–values (~2 ms) measured for this sample of slaughterhouse sludge, one can reasonably assume that this peak corresponds to the ^{1}H from organic matter. The remaining peaks in the range of ~6 ms up to 1 s can be associated with water strongly bound to the organic phase via vicinal water (hydrogen bound), with interstitial water physically trapped in bio-floc, by steric hindrance and with a small amount of water with higher mobility being less affected by the solid composition [43,44].

To assess the effect of specific solids on the T_2-distributions measured for this slaughterhouse wastewater, three samples were prepared: (i) distilled water; (ii) distilled water with chicken feather rachis and (iii) distilled water with chicken feather barb, proximal and distal barbule. The chicken feather was used as it was collected without additional purification by washing and/or sterilization. The measured T_2-distributions for these three samples are presented in Figure 3. It can be observed that the sample of distilled water (blue distribution) presents a single peak with the most probable T_2–value (maximum of peak) centered at 2.66 s. The T_2-distributions measured for distilled water samples with parts of chicken feather present three peaks: (i) the main broad peak (compared to the peak of pure distilled water) indicates an increased inhomogeneity of the aqueous medium; (ii) a small peak located between ~0.8 and 1.3 s placed in the subdomain of water with dissolved solids indicates that part of the feather impurities are dissolved in water and (iii) a small peak located between ~0.16 and ~0.23 s, indicates a less restricted mobility. This can be associated with water attached to chicken feather parts. This water may also experience a certain exchange with free water, therefore the real T_2–values may be affected by this exchange process [47]. As expected, due to smaller parts of feather, such as barb, proximal and distal barbule compared to rachis, the T_2-distributions measured for the first sample (top, red distribution in Figure 3) present broader peaks indicating a higher degree of inhomogeneity. Moreover, the position of the main peak is shifted towards smaller values indicating a reduction in the water mobility, most probably, by the interstitial water between barbs and barbules. In conclusion, these measurements demonstrates the effect of typical pollutants present in the chicken slaughterhouse wastewater, able to induce additional peaks at smaller T_2–values in the T_2–subdomains of water with undissolved solids (see Figure 2b), but also to shift the peaks located in the T_2–subdomains of water with dissolved solids towards smaller T_2–values.

The normalized T_2-distributions recorded for four types of slaughterhouse wastewater (untreated, chemically treated, biologically treated and discharged water, respectively) collected during months 2, 3 and 4 are presented in Figure 4. As expected, the main characteristics of these T_2-distributions are similar to those presented by samples collected in month 1, shown in Figure 2b, and discussed above. Nevertheless, the existence of some variability indicates the necessity for a statistical analysis of such samples. In this sense, for the T_2-distributions collected during months 2 to 4, one can remark: (i) the presence of two to three peaks for the untreated wastewater; (ii) the presence of one or no-peak for the chemically treated wastewater; (iii) two or three peaks for the biologically treated wastewater and (iv) just one peak for the discharged wastewater, which confirms the efficiency of the wastewater treatment applied.

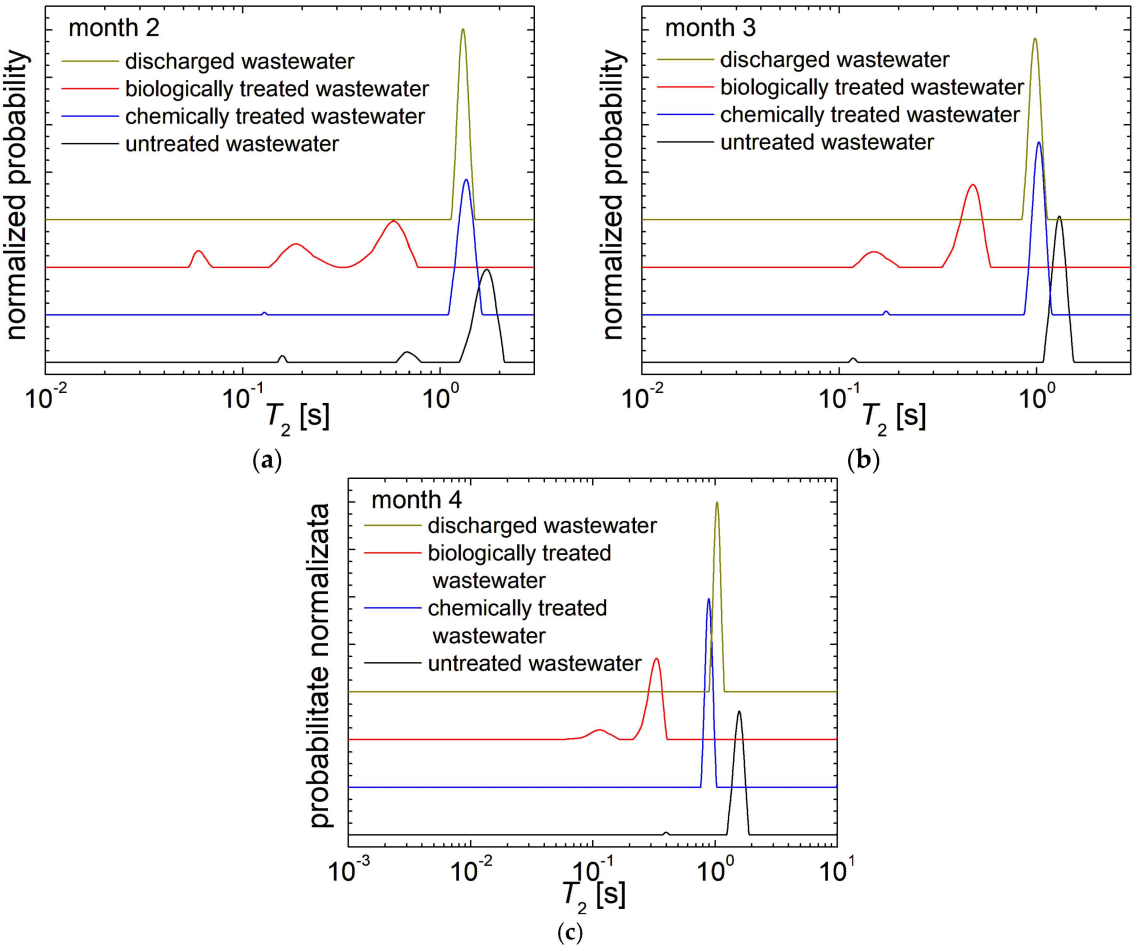

Figure 4. The normalized T_2-distributions recorded for the slaughterhouse wastewater: untreated (black), chemically treated (blue), biologically treated (red) and discharged wastewater (dark yellow) collected in (**a**) month 2; (**b**) month 3; (**c**) month 4.

Since the discharged wastewater presents only one peak, identified as the main peak located at the largest T_2-values, only the most probable values measured for this peak (here forth named $T_{2,1}$), associated with water containing dissolved solids, are comparatively presented in Figure 5a. This is the case for all four types of wastewater and sludge collected from the chicken slaughterhouse in all four months of monitoring. Relatively large variations are observed for this NMR parameter, especially in samples of biologically treated wastewater and sludge. The normalized T_2-distributions of the last one are presented in Figure S2 from Supplementary Information. The average values and the standard deviations calculated for those four months of observations are presented in Figure 5b). The largest value of average $T_{2,1}$ was calculated for the untreated wastewater (~1.54 s),

indicating a small number of dissolved solids in this samples. The relatively small standard deviation values indicate a certain consistency and homogeneity of these samples. The average value of $T_{2,1}$ calculated for the discharged wastewater (~1.22 s) has a relatively large standard deviation compared to the untreated wastewater samples. The larger variability presented by these samples can indicate the degree of the wastewater treatment efficiency. The average $T_{2,1}$ value for the chemically treated wastewater (~1.06 s) is calculated with a comparable relative measurement error. However, considering the large overlaps of error bar domains observed for discharged and chemically treated wastewater, one can say that this parameter cannot differentiate between these two types of wastewater. Among the wastewater samples, the biologically treated wastewater showed the smallest $T_{2,1}$ value (~0.66 s) and the largest standard deviations. This clearly indicates the presence of large amounts of dissolved solid in wastewater during the biological treatment stage. As expected, the smallest averaged $T_{2,1}$ value was calculated for the sludge (~0.33 s). For these samples the relatively large standard deviation values indicate their large variety. Since the untreated wastewater has an average $T_{2,1}$ value larger than that calculated for discharged wastewater, and due to the fact that the average value of $T_{2,1}$ calculated for chemically treated wastewater is, within the experimental error limit, comparable with that for the discharged wastewater, this parameter ($T_{2,1}$) alone is not a good indicator of water quality. Therefore, other parameters have to be considered, such as the ^{1}H NMR self-diffusion coefficient.

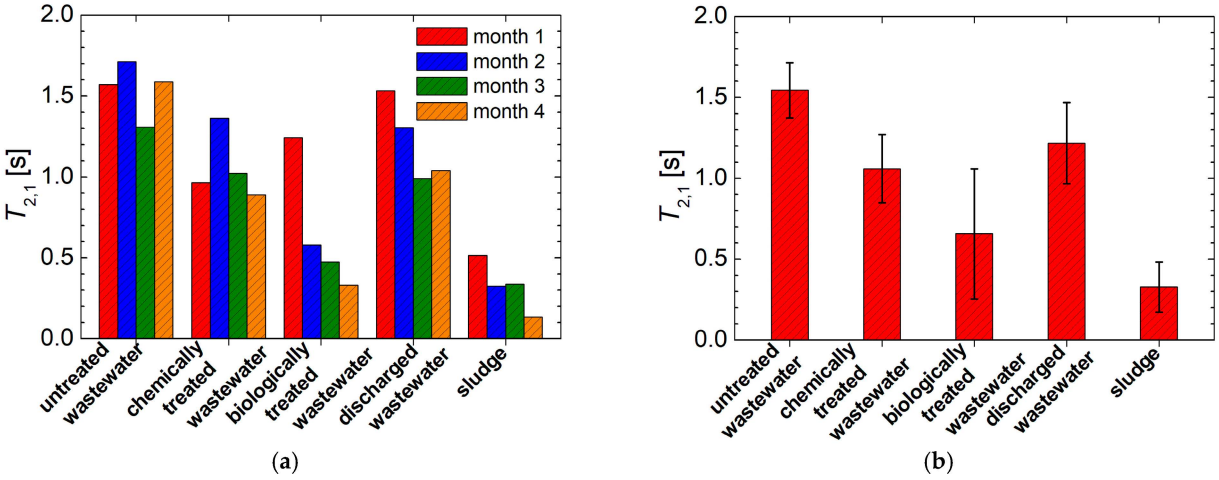

Figure 5. (**a**) The most probable T_2 values measured from the T_2-distribution as maximum of the main peak for all wastewater samples (untreated, chemically and biologically treated and discharged wastewater) and sludge collected from a slaughterhouse in months 1 to 4; (**b**) the average over all months of measurement of the most probable T_2 values presented in (**a**).

3.2. ^{1}H NMR Diffusometry of Wastewater and Sludge from Chicken Slaughterhouse

The ^{1}H NMR self-diffusion coefficient is a sensitive NMR parameter that can describe well the properties of fluids located in pores, capillaries, or in every case in which dissolved particles can influence the fluid molecules' mobility, as in our case. Figure 6a shows (on a logarithmic horizontal scale) the PGSE decays measured for all four types of slaughterhouse wastewater and sludge. As expected, the decay measured for sludge is characterized by the smallest diffusion (due to the strongest limitation of water molecules' mobility given by their interaction with large amounts of pollutants) observed as the slowest decaying curve. Such curves are hard to be interpreted quantitatively; therefore, a Laplace-like analysis is performed using the kernel presented in Equation (3). The normalized *D*-distribution functions resulting from this analysis are presented in Figure 6b. The domain of *D*-distributions had to be extended, compared to the normal domain for the self-diffusion coefficient [47]. This extension becomes reasonable by considering, as in the case of relaxation data (see Figure 2b), the split of *D*-distributions in two: (i) the first corresponding to the self-diffusion

of bulk water in the samples (see the blue background in Figure 6b) ranging for our samples from 10^{-9} m^2/s up to (an arbitrary) 10^{-8} m^2/s; (ii) the second associated to water molecules attached to solid residues and transported by flotation and sedimentation, having therefore a larger apparent diffusion coefficient in the range of 10^{-8} m^2/s up to 10^{-6} m^2/s. In this case, the limit of separation between the real self-diffusion coefficient and the apparent diffusion coefficient, describing a flow rather than a self-diffusion process, was chosen as a convenient route between these two domains.

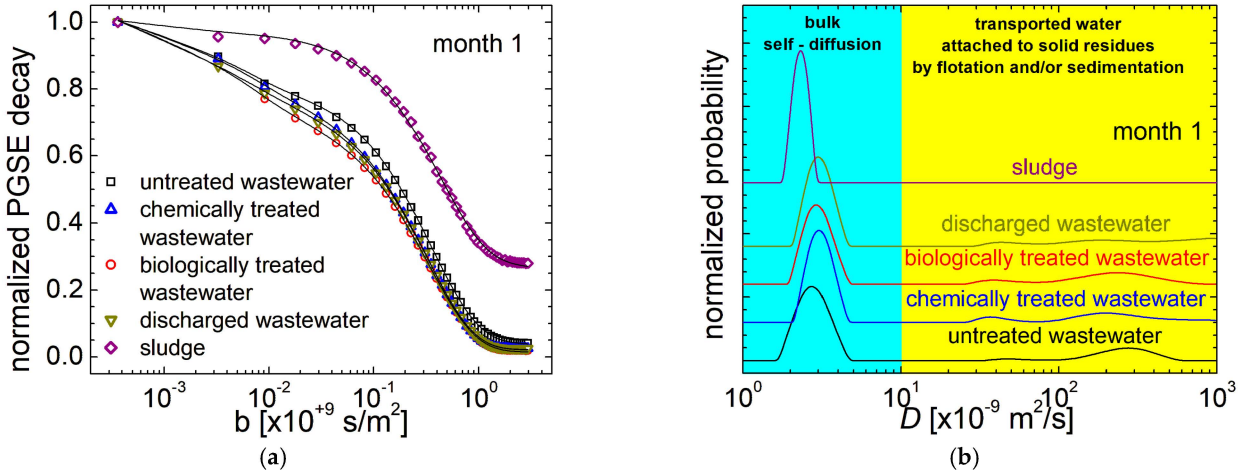

Figure 6. (**a**) The normalized PGSE decays recorded for the slaughterhouse wastewater (untreated—black square, chemically treated—blue upper triangle, biologically treated—red circle and discharged wastewater—dark yellow lower triangle) and sludge collected in month 1; (**b**) the normalized *D*-distributions of the PGSE decay curves presented in (**a**).

All samples present the largest amount of water as bulk water characterized by the largest peak in the self-diffusion coefficient distribution (Figure 6b). For the first month of monitoring, the wastewater samples (untreated, chemically and biologically treated and discharged wastewaters) presented three peaks, the largest, as mentioned, in the domain of self-diffusion and two of them in the domain of transported water. It is natural to assume that the largest transport coefficient should be associated with water characterized by a large velocity, and therefore a large mobility, specific to the small particles that the water is attached to. On the contrary, if the water molecules are attached to large particles, the mobility of this water-particle system is small. Therefore, the mobility of attached water is small and it is observed as a small apparent diffusion coefficient. The untreated wastewater leads to a broad peak centered at 2.76×10^{-9} m^2/s. This becomes narrow as a result of the purification process that reduces the samples' heterogeneity. A narrow peak was also measured for the sludge sample. The most probable self-diffusion coefficient (the peak maximum) increases from 2.76×10^{-9} m^2/s measured for untreated samples of wastewater to 2.76×10^{-9} m^2/s to 2.98×10^{-9} m^2/s for discharged wastewater, indicating an increased mobility (or reduced restrictions). A large value is obtained for chemically treated wastewater (3.03×10^{-9} m^2/s). The lowest most probable self-diffusion coefficient was measured for sludge (2.31×10^{-9} m^2/s). This is normal, since this sample contains the largest amount of residue. For the first month of monitoring, the *D*-distributions for sludge present no peaks in the domain of transported water. This is not due to the fact that there are no residues but, on the contrary, may be due to the fact that the amount of residue is so large that the mobility of water molecules, due to the sedimentation or flotation processes, is strongly reduced. For months of monitoring 2–4, the *D*-distributions measured for sludge samples presented similar peaks in the water transport domain (see Figure S3 from the Supplementary Information).

Two broad peaks with small amplitude are observed for all the wastewater samples in the transported water domain (Figure 6b—yellow background). In all cases, the integral

area under the peaks corresponding to water molecules attached to small particles (the larger D-values, often of the order of hundreds of 10^{-9} m^2/s) is larger than the integral area of peaks corresponding to water molecules attached to large particles (the small D-values, often of the order of tens of 10^{-9} m^2/s). This indicates the presence of larger numbers of small particles in the slaughterhouse wastewater. The largest number of such small particles was found in untreated wastewater, as expected. The measurement of self-diffusion coefficient distributions for the discharged wastewater (Figure 6b) revealed peaks in the domain of transported water. This was a surprise, given that, for the relaxation times' T_2-distributions, the discharged wastewater generated a single peak (see Figures 2b and 4). The presence of several peaks in the D-distributions measured for discharged wastewater associated with water attached to mobile particles indicates that the ^{1}H NMR measurement of the self-diffusion coefficient is a more sensitive method than ^{1}H NMR relaxometry. The area under these peaks indicates the presence of a small number of such particles in the discharged wastewater. This probably has the same (or appropriate) relaxation time T_2 as the bulk water, therefore cannot be distinguished by the ^{1}H NMR relaxometry method. The peaks measured in the transported water domain are broad, indicating a large heterogeneity of samples, here translated into a large distribution of particle dimensions. Moreover, the presence of two resolved peaks (instead of just one really broad peak) suggests the presence of at least two types of particles with different origins.

The normalized self-diffusion D-distributions measured for all chicken slaughterhouse wastewater samples collected in months 2, 3 and 4 of monitoring are presented in Figure 7. Generally, the characteristics previously described for month 1 of monitoring are also valid for these samples. One can remark: (i) the similarly small deviation of the most probable self-diffusion coefficient (measured at maximum of peaks from D-distributions) that from here will be labeled as D_1; (ii) the large amount of water attached to small particles especially for untreated wastewater, chemically treated wastewater and discharged wastewater; (iii) a comparable or small amount of water attached to small particles (D of the order of hundreds of 10^{-9} m^2/s—from now labeled as D_3) than those attached to large particles (D of the order of tens of 10^{-9} m^2/s—from now labeled as D_2).

The measurement parameters (magnetic field gradients and delays in the PGSE pulse sequence—see Figure S1b from the Supplementary Information) are calibrated for good measurement of the bulk water self-diffusion coefficient. For our samples, this parameter (D_1) is measured with the largest precision (affecting the full decay curve—see Figure 6a) compared with the apparent diffusion coefficients D_2 and D_3. The latter two are measured with a small precision since, being one or two orders of measurement larger (than D_1), can only affect fewer points at the beginning of the decay PGSE curve.

For a quantitative analysis of the purification process via self-diffusion, only the D_1 diffusion coefficient will be considered. All D_1 values measured for all four types of wastewater samples and sludge for all four months of monitoring are comparatively presented in Figure 8a. With some exceptions (month 2 for untreated wastewater and biologically treated wastewater, and month 1 for chemically treated wastewater, discharged wastewater and sludge), the measured values of the most probable self-diffusion coefficient D_1 are similar for the other three months. The average of all four months and the measurement errors are presented in Figure 8b. Within the experimental error limit, one can observe that the D_1 parameter can be used to differentiate between the types of wastewater. An overlap only exists between the chemically treated wastewater and the discharged wastewater. The smallest D_1 value (and the largest error) was measured for sludge, and the largest were measured for chemically treated wastewater and for discharged wastewater. In conclusion, the large value measured of the self-diffusion coefficient D_1 for discharged wastewater indicates a small restriction of the water molecules' mobility and therefore a good efficiency of the wastewater purification applied in the chicken slaughterhouse.

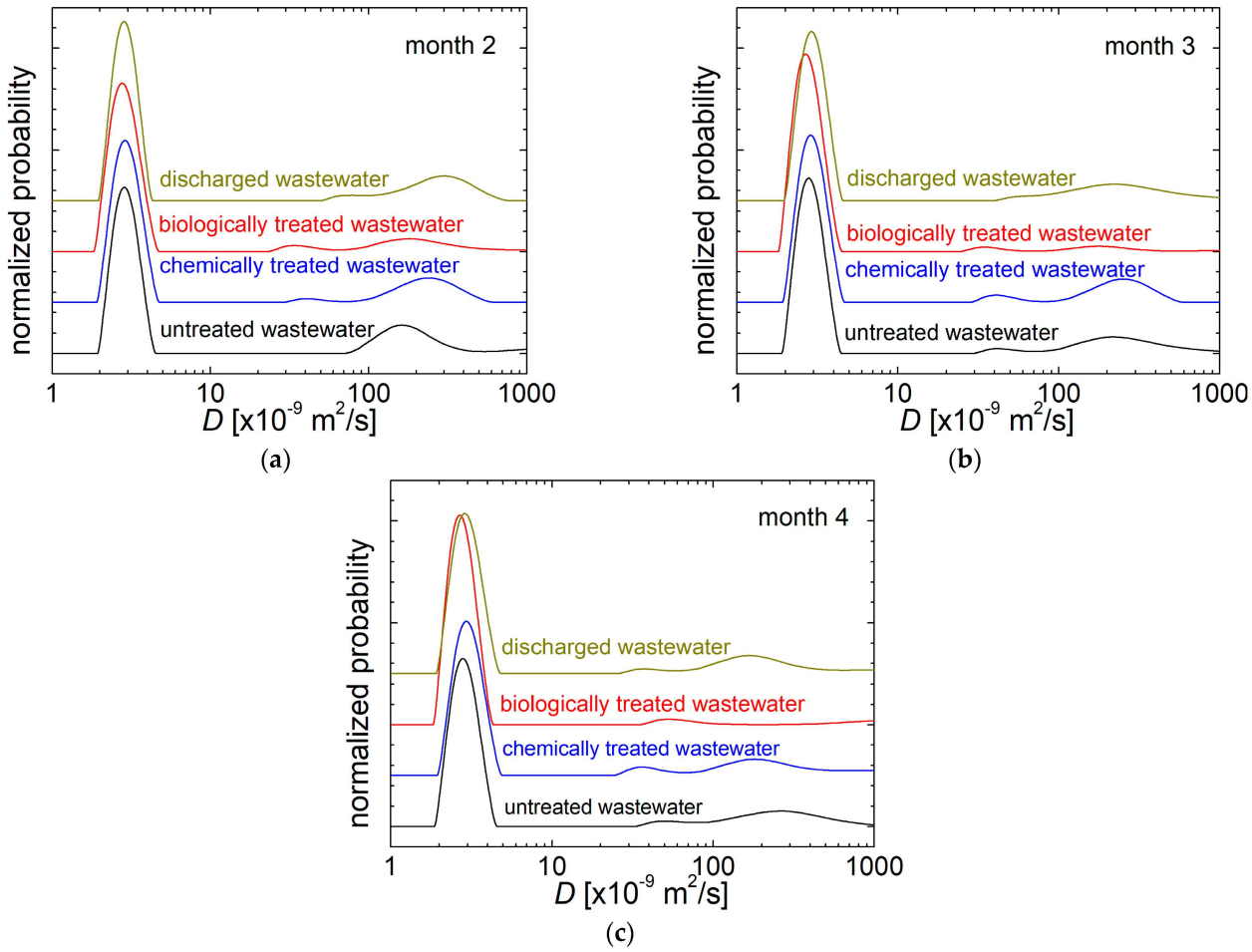

Figure 7. The normalized *D*–distributions recorded for the slaughterhouse wastewater: untreated (black), chemically treated (blue), biologically treated (red) and discharged wastewater (dark yellow) collected in (**a**) month 2; (**b**) month 3; (**c**) month 4 of monitoring.

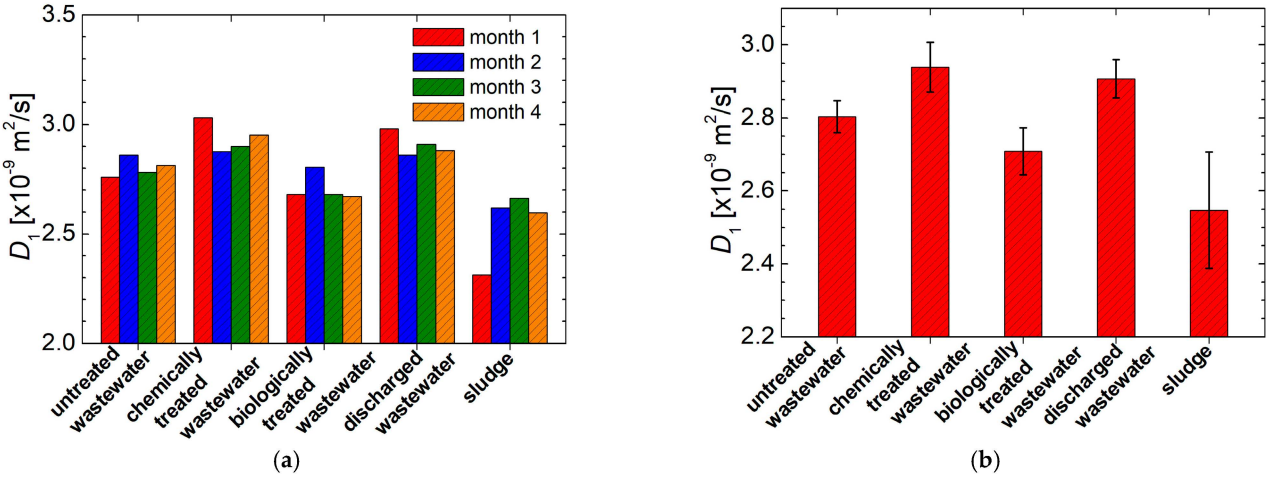

Figure 8. (**a**) The most probable self-diffusion coefficient D_1 values measured from the *D*–distribution as maximum of the main peak for all wastewater samples (untreated, chemically and biologically treated and discharged wastewater) and sludge collected from a slaughterhouse in months 1 to 4; (**b**) the average over all months of measurement of the most probable self-diffusion coefficient D_1 values presented in (**a**).

3.3. VIS-NearIR Spectroscopy

Both ^{1}H NMR relaxometry and diffusometry, as previously discussed, show that even in the discharged wastewater from chicken slaughterhouse, there is a variety of particles visible or invisible to the naked eye. These particles will affect (by absorption) the visible light that eventually passes through wastewater. The classical method largely used to quantify the amount of such particles is by determining its turbidity [3]. This is a global parameter, giving a single value for a specific sample. We propose to replace the turbidity measurement by acquiring a VIS-nearIR spectrum.

An example of such VIS-nearIR spectra recorded for untreated wastewater (after 30 min of sedimentation), chemically treated wastewater, biologically treated wastewater (after 10 min of sedimentation), discharged wastewater and sludge (1 mL of sludge distilled in 20 mL of distilled water and then measured after 5 min of sedimentation) for samples collected in month 1 of monitoring, are presented in Figure 9. The array sensor of Pasco VIS-nearIR spectrometer allowed us to record the spectra in seconds, therefore, the sedimentation and/or flotation process will not affect the spectral amplitude function of wavelength. This was a problem when a similar measurement was attempted using a step-by-step UV-VIS spectrometer, when the measurement is performed by gradually changing the wavelength, and then the measurement lasted for several minutes. All wastewater and sludge solution present a large absorption in violet light (possible extended in the ultraviolet domain). One can also observe a certain absorption at the wavelength of ~420 nm, then the discharged wastewater, chemically and biologically treated wastewater present a certain decay of the absorbance with the increasing the light wavelength. For these samples, one can observe a certain absorption doublet in the infrared domain at wavelengths larger than 900 nm. For the untreated wastewater, one can observe an additional relative maximum of absorption at λ~560 nm at a so called Chartreuse color between green and yellow. Similar features are observed in sludge solution and in untreated wastewater, except for the fact that the absorbance through the sludge solution is not decaying for wavelengths larger than 560 nm up to ~840 nm that belong to the near infrared domain.

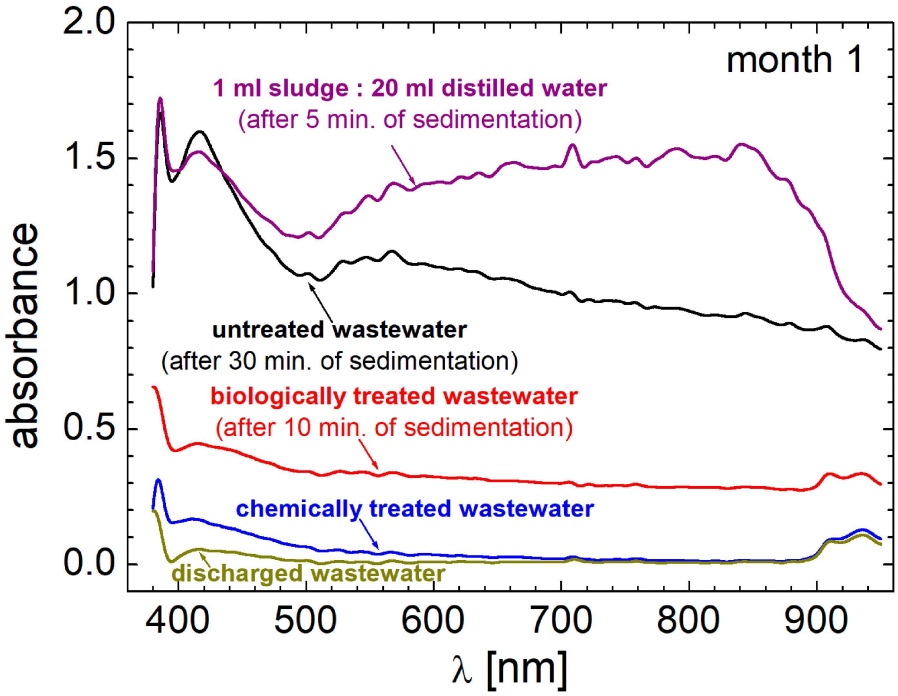

Figure 9. The VIS-nearIR absorbance measured for the chicken slaughterhouse wastewater and 1 mL of sludge residues distilled in 20 mL of distilled water collected in month 1 of monitoring.

An extensive analysis can be performed of the light absorption function of wavelength correlated with the particles sizes and types of pollutants. Such analysis is beyond our scope, therefore will not be discussed here. Nevertheless, it is important to observe that the VIS-nearIR spectroscopy is sensitive to the degree of pollution of wastewater, presenting the largest absorbance for the sludge (even if it was diluted 1:20 in distillated water) and then for the untreated wastewater. Next, less absorbance was measured for the biologically treated wastewater (since it was collected before sedimentation). A small absorbance was measured for chemically treated wastewater and the cleanest wastewater was found the discharged wastewater. Among of all our methods, it is the VIS-nearIR spectroscopy that more accurately reveals the purification process. Unfortunately, this method also can be affected by large errors, as moving particles enter (by sedimentation and/or flotation) between the LED light source and detector, and by data sampling. Going back to a single parameter aimed to characterize the VIS-nearIR spectra, we found the total absorbance, i.e., the integral area under each spectrum. This parameter (in arbitrary units) is presented in Figure 10a for all wastewater samples and sludge and for all four months of monitoring. Large variations can be observed in untreated wastewater, biologically treated wastewater and sludge. The statistical average of the total absorbance and the measurement errors are presented in Figure 10b. Large error bars are observed for the samples enumerated before. One can remark the small values for the averaged total absorbance measured in chemically treated wastewater and in discharged wastewater. This is a new proof that the wastewater purification process applied at the chicken slaughterhouse is efficient. We also performed a correlation/calibration measurement for some milky-like samples over a wide range of turbidity degrees, and we found that the total absorbance measured from VIS-nearIR spectra can replace the turbidity measurement with a proper calibration, since the dependence in the domain 0–500 ntu is linear. Over this limit of 500 ntu, there is a non-linear relationship. The resulted calibration curve is given in Figure S4 in Supplementary Information. Finally, the large variation of data in VIS-nearIR spectra can be reduced by multiple sampling and an appropriate statistical average.

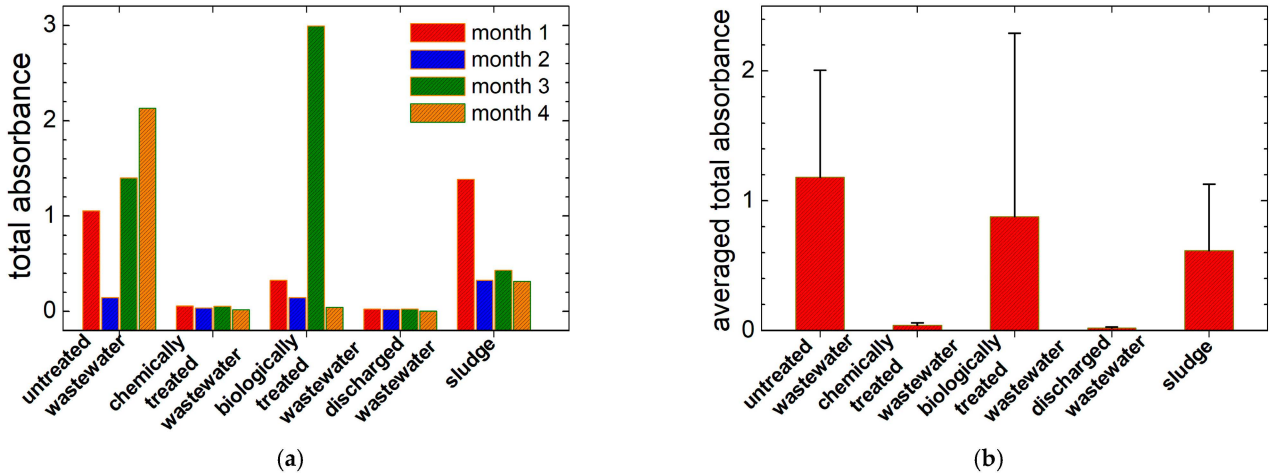

Figure 10. (**a**) The total absorbance of VIS-nearIR spectra recorded for the slaughterhouse wastewater (untreated, chemically treated, biologically treated and discharged water) and sludge collected in all four months of monitoring; (**b**) The averaged of total absorbance of VIS-nearIR spectra of wastewater and sludge presented in (**a**).

3.4. The pH Measurements

A widely used parameter for water testing is its pH. The wastewater pH values for all samples (untreated, chemically and biologically treated, discharged wastewater and sludge solution) collected in all four months were measured and are shown in Figure 11a. Large variations can be observed among samples collected in different months. One can remark a minimum value for pH of ~5.1 and a maximum value of ~8.4, both being measured

for samples collected in month 1 of monitoring. Interesting results are obtained for the average values calculated for all four months of monitoring. These values are presented in Figure 11b together with the statistical measurement errors. The average pH values can be found between ~6.5 for discharged wastewater and ~6.8 for chemically and biologically treated wastewater. Nevertheless, within the experimental error limits (the maximum pH error was calculated for chemically treated wastewater at approximately ±1), one cannot distinguish the samples by measuring the pH parameter. Even the sludge solution (the sludge pH was measured for the solution prepared for the VIS-nearIR spectroscopy) has a pH between the same limits. One also observes that the pH was a controlled parameter for the chemically treated wastewater, and its value measured for the wastewater automatically opens the valves of the coagulant, NaOH and liquid polymer tanks.

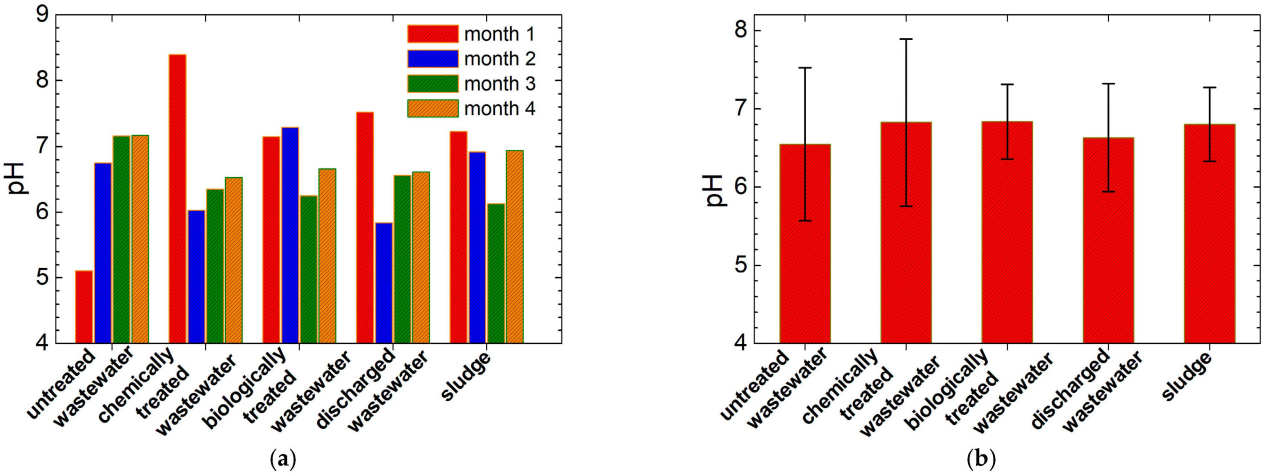

Figure 11. (**a**) The pH measured for the slaughterhouse wastewater (untreated, chemically treated, biologically treated and discharged wastewater) and sludge collected in all four months of monitoring; (**b**) The averaged pH over months measured for all four wastewater and sludge samples presented in (**a**).

3.5. Electrical Conductivity Measurements

The dissolved and undissolved pollutants will change the electrical conductivity (EC) of slaughterhouse wastewater. Figure 12a presents the measured values for all types of wastewater and sludge (in solution as was prepared for VIS-nearIR spectroscopy) collected in all four months of monitoring. As in the case of pH measurements, large differences of the electrical conductivity values can be observed when comparing samples collected in different months. (The average values together with the standard deviations are presented in Figure 12b). In general, for the same type of dissolved particles, a large value measured for the electrical conductivity implies a large concentration of pollutants. The average values of electrical conductivity σ show a decay when comparing untreated wastewater to chemically and biologically treated wastewater. This showed similar values of σ, while the discharged wastewater is characterized by the smallest σ value. Contrary to pH, in the case of electrical conductivity, the value measured for sludge is substantially larger compared to the values measured for all the types of wastewater. Examining the magnitude of error bars, the first idea is that the electrical conductivity, despite the average values, cannot be used to discriminate between different kinds of wastewater. On the contrary, as we will see in the subchapter dedicated to statistical analysis of principal components, not only can the electrical conductivity be successfully used in differentiation between all four types of wastewater but. together with total dissolved solids, it proves to be an important parameter.

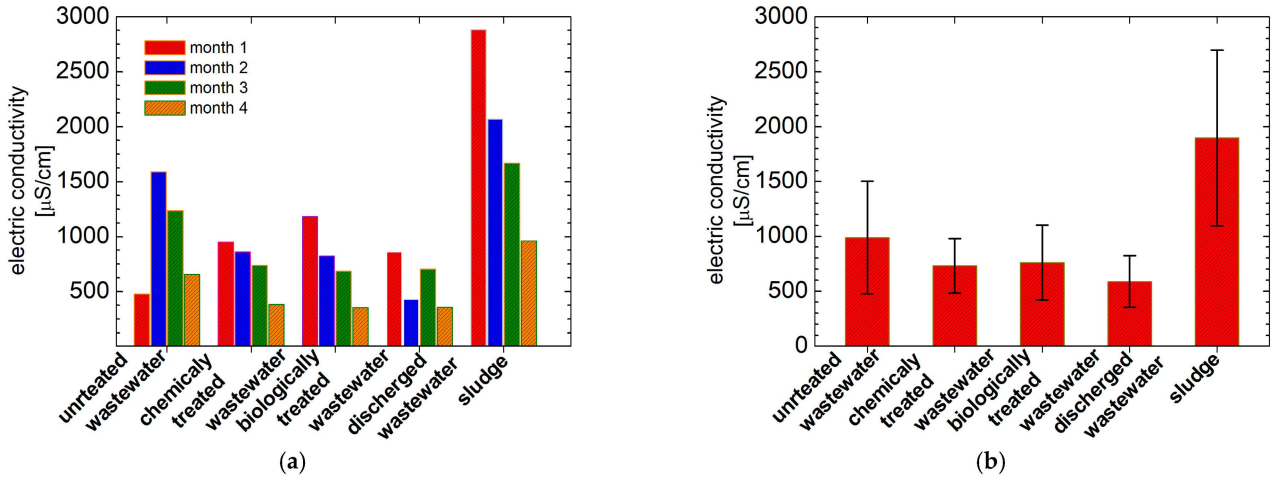

Figure 12. (**a**) The electrical conductivity (EC) measured for the slaughterhouse wastewater (untreated, chemically treated, biologically treated and discharged wastewater) and sludge collected in all four months of monitoring; (**b**) the average EC over months measured for all wastewater and sludge presented in (**a**).

3.6. Total Dissolved Solids' Measurements

A total dissolved solid is a global parameter that, as in the case of electrical conductivity, is usually applied for the characterization of the pollution degree in wastewaters, in particular for those collected from chicken slaughterhouses. In fact, often these two parameters are well correlated. This is a feature that was also observed for our samples. In Figure 13a, the measurement of TDSS values are presented for all the wastewater samples (untreated, chemically and biologically treated and discharged wastewater) and sludge, for all four months of monitoring. With some minor differences, these values look similar to those measured for the electrical conductivity (see Figures 12a and 13a). As in the case of electrical conductivity, the TDSS values are out of range for samples collected in month 1 of monitoring for untreated wastewater, biologically treated wastewater and sludge. Contrary to the measurement of EC in the case of TDSS for month 4 of monitoring, the data seem to be in the same range with the other values measured for the samples collected earlier. The average TDSS values and the measurement errors are comparatively presented in Figure 13b. A large value is obtained for the untreated wastewater (~585 ppm). Similar values are obtained for chemically and biologically treated wastewater (427.75 ppm and 426.5 ppm, respectively). As a result of purification, the discharged wastewater has an average value of TDSS of ~392.5 ppm. The relative elevated value of TDSS measured for the discharged wastewater is in agreement with the ^{1}H NMR diffusometry measurements (Figures 6b and 7), VIS-nearIR spectroscopy (Figure 9), and electrical conductivity (Figure 10), which all showed that the discharged wastewater is not pure, contrary to the interpretation of ^{1}H NMR relaxometry data (Figures 2a and 4). Moreover, it will be shown later than the TDSS measurements are important data for discrimination between different types of wastewater and sludge via statistical analysis of the principal components.

3.7. Principal Component Analysis

The method by which one can analyze variate data types characterized by variables with different measurement units is that of statistical multivariate analysis, in particular the analysis of the principal components [53,54]. For our analysis, we implemented numerically our own analysis program written in MatLab and we plotted the results using Microsoft Excel. The data were verified using PAST Version 3.25 which stands for PAleontological STatistics software and Origin 2022b (Academic). For the principal component analysis we produced an input data matrix with the most relevant parameters (a total of six), as listed in Table 1. As variables, we selected: (i) the total absorbance as measured from VIS-nearIR spectra (see Figure 9); (ii) the $T_{2,1}$ spin–spin relaxation time values measured as the most

probable value for the water with dissolved solids (see Figures 2b and 4); (iii) the self-diffusion coefficient D_1 values corresponding to bulk water measured as the most probable coefficient from the maximum of D-distribution (see Figure 6b); (iv) the pH (see Figure 11a); (v) the electrical conductivity, EC (see Figure 12a) and (vi) the total dissolved solids (see Figure 13a). These values are listed for all types of wastewater (untreated, chemically treated, biologically treated and discharged wastewater) and sludge which are considered to represent a particular group, and all four months of monitoring are considered as particular variations in each group. In total, the matrix contains 6 columns (representing the independent parameters) and 20 rows (representing the number of measured data for each parameter). Since the number of independent parameters is smaller than the number of data items, then this will give the number of principal components (PCs). Therefore, in our case the number of PCs was six. The analysis is similar to that in an eigenvectors/eigenvalues problem. The proportion with the contribution of each component and the cumulative proportion are presented in Figure S5a from the Supplementary Information. One can see that the first component (PC1) can explain ~48.9 of the variation in the experimental data. If the PC2 is also considered, then ~69.3% of the variations can be explained. In order to pass over 90%, PC3 and PC4 must also be considered. The eigenvalue functions of the PC number are presented in Figure S5 from the Supplementary Information.

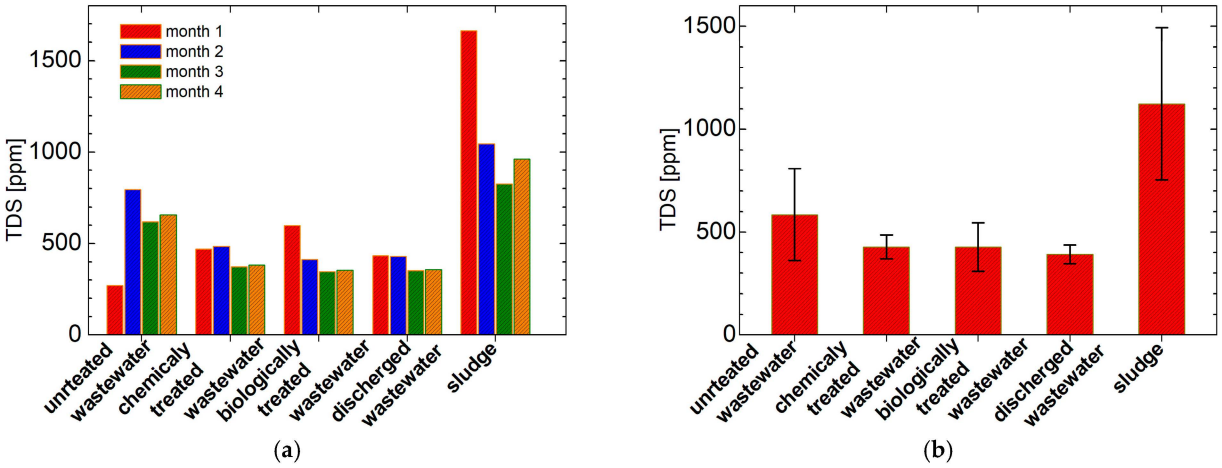

Figure 13. (**a**) The total dissolved solid (TDSS) measured for the slaughterhouse wastewater (untreated, chemically treated, biologically treated and discharged wastewater) and sludge samples collected in all four months of monitoring; (**b**) the average TDSS measured for all wastewater and sludge samples presented in (**a**).

4. Discussion

Principal component analysis is a powerful tool to assess the statistical behavior of measured data, allowing discrimination between different parts of a statistical system, to find correlations between different types of parameters and, if relevant, to observe an evolution process [54]. The main result of the application of PCA analysis on our slaughterhouse wastewater measurements is presented in Figure 14 as a plot of PC2 (second principal component) in correspondence with PC1 (the first principal component). The data must be analyzed in close relationship with the results listed in Table 2. Here, the contributions of each parameter (the total absorbance of VIS-nearIR spectra, $T_{2,1}$ spin–spin relaxation time, the self-diffusion coefficient D_1, pH, EC and TDSS) to the principal components PC1 to PC6 are given. To assess the importance of a specific parameter for each principal component, only the magnitudes of listed values must be considered. The sign of listed values will contribute to the displacement of data presented in Figure 14 and will lead to the separation between different types (groups) of samples. The first principal component PC1 is characterized by the largest separation of data, and the displacement

(variation) decays with the increase of principal component number, PC6 having the smallest displacement.

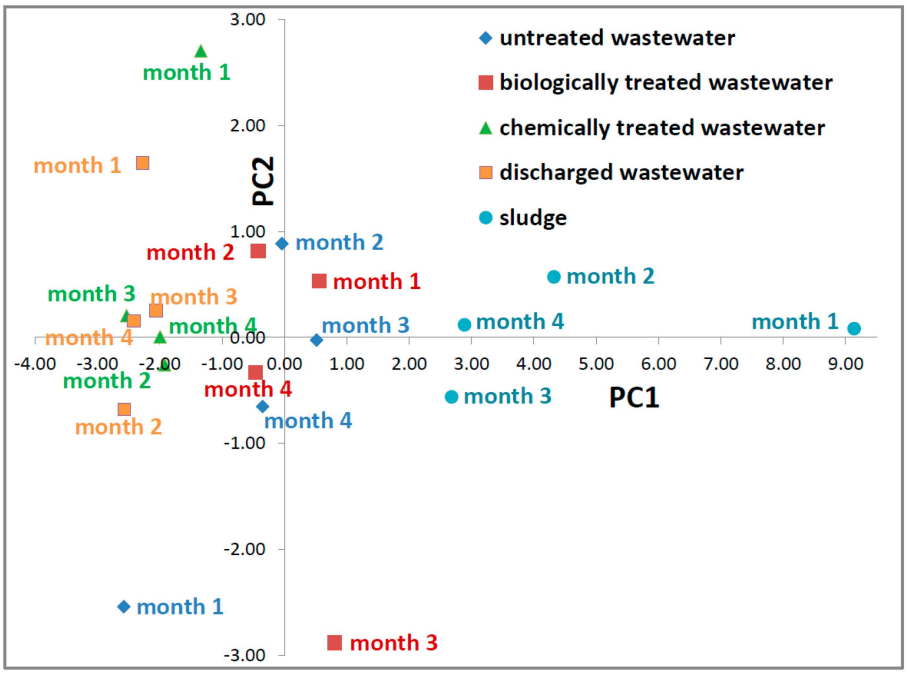

Figure 14. The main PCA analysis: the 2D plot of PC1 function of PC2 for the slaughterhouse wastewater (untreated, biologically treated, chemically treated and discharged wastewater) and sludge samples collected in all four months of monitoring.

Table 2. The contribution of relevant parameters (total VIS-nearIR absorbance, the most probable transverse relaxation time $T_{2,1}$, the self-diffusion coefficient D_1, pH, electrical conductivity EC and the total dissolved solids TDSS) measured for the slaughterhouse wastewater to the principal components PC1–PC6.

Parameter	PC1	PC2	PC3	PC4	PC5	PC6
total VIS-nearIR absorbance	0.336	−0.627	0.550	0.430	−0.079	−0.025
$T_{2,1}$ [s]	−0.561	0.054	0.703	−0.417	0.117	0.026
D_1 [10^{-9} m^2/s]	−0.892	0.343	0.122	0.036	−0.244	−0.104
pH	0.250	0.794	0.264	0.478	0.085	0.032
EC [μS/cm]	0.884	0.220	0.173	−0.288	−0.211	0.118
TDSS [ppm]	0.933	0.165	0.107	−0.226	0.042	−0.195

Note: In all cases, the measurement errors are smaller than 5%.

A PCA statistical analysis is considered to be successful (the number and the type of chosen parameters is relevant, the data are correlated, etc.) if the data presented in a two- (as in the case of the plot in Figure 14) or a multi-dimensional space presents a cluster behavior [49,50]. This means that the points representing the data from the same group are found together and as far away as possible from other groups. Analyzing real data, affected by many types of errors, one can find overlapping regions between different groups and often there will be point(s) that are missed (located away) from a designated group.

In Figure 14, the group of four points (month 1 to four of monitoring) corresponding to untreated wastewater is shown with a blue diamond. For months 2, 3 and 4, these points are located towards the center of the figure having the smallest PC1 and PC2 values. The point corresponding to month 1 of monitoring for untreated wastewater is located at a large negative PC1 and PC2. Table 2 summarizes the main contributions to PC1: the global parameters TDSS (0.933) and EC (0.884), and the specific NMR self-diffusion coefficient

D_1 (−0.892). A certain contribution can be found from the $T_{2,1}$ NMR parameter (−0.561). The smallest contribution to PC1 comes from pH (0.25) and total absorbance in VIS and near IR (0.336). Conversely, the main contribution to the second principal component PC2 comes from pH (0.794). In addition, a large contribution can be credited the total VIS-nearIR absorbance (−0.627). To PC2, an insignificant contribution comes from $T_{2,1}$ (0.054), followed by TDSS (0.165) and EC (0.22). The NMR self-diffusion coefficient D_1 will make a relatively important contribution (0.343). Therefore, the measurements of pH, EC and TDSS performed for samples collected in month 1 of monitoring are out of range. A similar behavior can be found for biologically treated wastewater (red filled square in Figure 14). Here, the points corresponding to samples collected in months 1, 2 and 4 are grouped and the point corresponding to month 3 is largely displaced in the negative direction of PC2. Therefore, the pH value and the total absorbance in VIS-nearIR measured for this sample are the main factors responsible for this out of group position. Grouped at negative values of PC1 can be found the points belonging to chemically treated wastewater (shown with filled green triangles) and discharged wastewater (filled yellow square). Especially in PC1, one can observe a good grouping behavior with only a small variation. From the point of view of PC1, the biologically treated wastewater (PC1: from −0.46 to 0.81—without month 3) is the most similar to the untreated wastewater (PC1: from −2.53 to −1.92—without month 1), while the discharged wastewater (PC1: from −2.57 to −2.06) is the most different from untreated wastewater. From the point of view of the purification process, this is a very good observation. One can extend this kind of analysis. By taking a look at the cluster of discharged wastewater, one can see that the chemically treated wastewater (for months 2, 3 and 4) will have similar properties to those of the discharged wastewater. From the point of view of PC1, the chemically treated wastewater (PC1: from −2.53 to −1.92—without month 1) collected in month 3 of monitoring is cleaner (different from untreated wastewater) than the discharged wastewater collected in months 3, 1 and 4. However, if the data are well grouped in PC1, the points representing the properties of samples collected in month 1 of monitoring for chemically treated and discharged wastewater, in PC2, are away from the group center of gravity. For the most part, the pH measured for these samples (of chemically treated wastewater and discharged wastewater) led to this displacement.

A completely opposed behavior is observed for sludge (blue circles). The group with these samples is localized at positive large values of PC1, well separated even from untreated wastewater. In the second component, one observes that the values are distributed around the zero value of PC2. Then, one can conclude that PC1 can be used to successfully separate the wastewater according to is purity. The most contaminated sample was the sludge sample, collected in month 1 of monitoring, and the cleanest wastewater was the wastewater sample collected in month 2 of monitoring. Another study based on FT-IR spectroscopy supports this conclusion [9]. For our wastewater system (also containing the sludge), one can see that the most significant parameters were (in order): (i) the total dissolved solids TDSS; (ii) the self-diffusion coefficient D_1; (iii) the electrical conductivity EC; (iv) the transverse relaxation time of dissolved solids $T_{2,1}$. The most irrelevant parameter was pH. Nevertheless, pH and the total absorbance in VIS-nearIR are important parameters capable of identifying samples (in PC2) from the same group with properties away from the average expectation.

Another important result of our PCA assay is the degree of correlation between all parameters considered in pairs. In the case of wastewater collected from a chicken slaughterhouse, the most correlated parameters were found to be the electrical conductivity, EC, and the total dissolved solids, TDSS. This is not a surprise, since the physical support for electrical conductivity is given by dissolved solids, as distilled water presents poor electrical conductivity. Considering the elements of covariance matrix C (using the MatLab 2020 numeric program, but not from PAST software), and that the eigenvector and eigenvalue problems were solved, a large value can be seen for the elements (there are two symmetrical elements around a main diagonal that have values of 1, meaning that each parameter is perfectly correlated with itself) corresponding to the EC and TDSS parameters. However,

the values are not as large as expected. To understand this, in Figure 15, the TDSS is plotted as a function of EC. Now, the correlation coefficient can be better understood. The first observation is that, indeed, the TDSS is well correlated to the EC parameter but, in our case, for all samples collected from the chicken slaughterhouse in four months of monitoring, there are two linear dependences rather than a single one. With one exception, one can see that the data (TDSS and EC) measured for months 1, 2 and 3 of monitoring for untreated, chemically and biologically treated wastewater discharged wastewater and sludge are in a very good linear correlation. In addition, the data collected in the four months of monitoring are arranged in a second linear dependence. Usually, such double linear correlations can be explained: (i) by a change in the treatment process (to include different types of particles with a different electrical behavior); (ii) by a change in dissolved pollutants; (iii) by both causes. In our case, the most probable cause is the fact that the wastewater samples collected in month 4 of monitoring of wastewater were used in the processing of different kinds of chicken (with different origin, size, age, etc.) An interesting observation is the fact that the point corresponding to the discharged wastewater collected in month 2 is placed on the short dependency belonging to month 4.

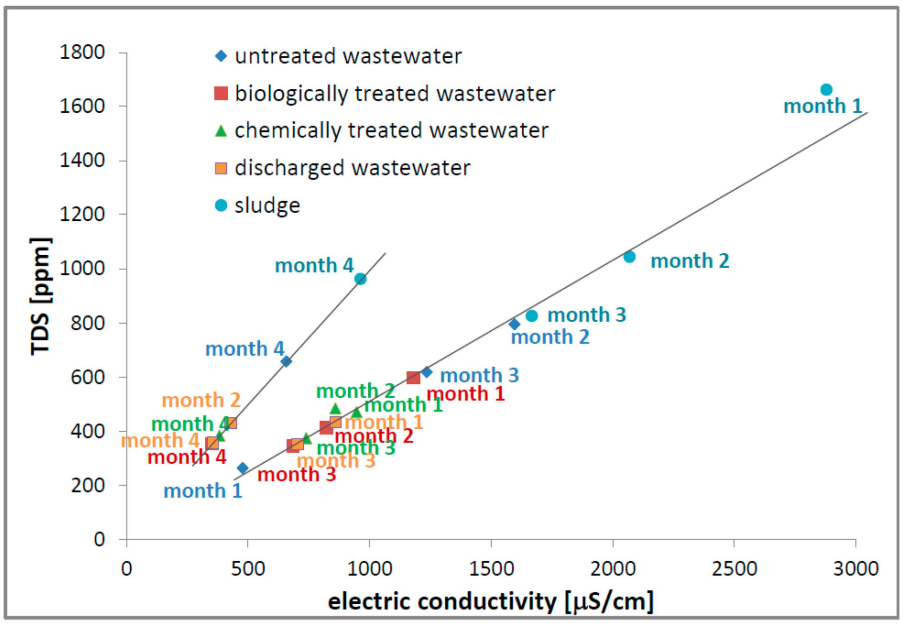

Figure 15. The double linear correlation between electrical conductivity (EC) and totally dissolved solids (TDSs) for the wastewater and sludge.

In the recent times, artificial intelligence is used in more and more fields, from entering parking places to cancer prediction [54]. This is useful, especially in cases where the classes/categories are not well isolated, superposition between them exists and a probabilistic based decision has to be considered. In this sense, we developed a dedicated program written in JavaScript (JS–version 2024) that used an online library named ML5 [55,56] to easily build an Artificial Neural Network. This is used to predict the probability that a new measurement of all parameters analyzed by PCA will be classified as untreated wastewater, chemically or biologically treated wastewater, discharged wastewater, or sludge (see Figure 16). We simulated the incidence of such analysis in every element of a 100 × 100 matrix associated with the 2D plot of the main PCA analysis (see Figure 14). Prior to that, the JS loaded the 5 × 4 = 20 values of PC1 and PC2 coordinated, together with the label associated with our five types of samples (four wastewater and sludge). The ANN was trained for 10,000 epochs with a learning rate of 10% and the trained model was saved to be loaded anytime needed (without any new training, which is a time-consuming procedure). Once the trained model is loaded, it can be used to generate prediction related to the probability that, in a chosen position (in the main analysis 2D space) resulting from

a PCA analysis of a new element, the sample is associated with one of the trained labels (i.e., untreated wastewater, chemically treated wastewater, biologically treated wastewater, evacuated wastewater or sludge). The generated prediction maps, which simplify the PCA analysis even further, are presented in Figure 16. Thus, Figure 16a presents the predicted probability (measured from 0 to 1, where 1 represents 100%) for untreated wastewater. One can observe that the maximum probability is obtained for PC1 and PC2 negative (see also Figure 14), especially due to the sample collected in month 1. A relative maximum (around 50%) is obtained for PC1 and PC2 values close to zero. especially due to the samples collected in months 2 and 3. The PCA analysis of chemically treated wastewater can be found with high probability (>70%) if PC1 is between −3 to −1 and PC2 is larger than 1 (see Figure 16c). A high probability of association, in the PCA analysis, between the measured result with biologically treated wastewater is to have PCA between −1 and 0, and PC2 with large positive or negative values (see Figure 16c). From Figure 16c, one can see that a smaller PC1 value (almost independent of PC2 value) is associated with the discharged wastewater (see Figure 16d). Values of PC1 larger than zero can be associated with high probability to measured sludge (see Figure 16e). The prediction maps can offer enhanced representation of sample classification related to the PCA analysis.

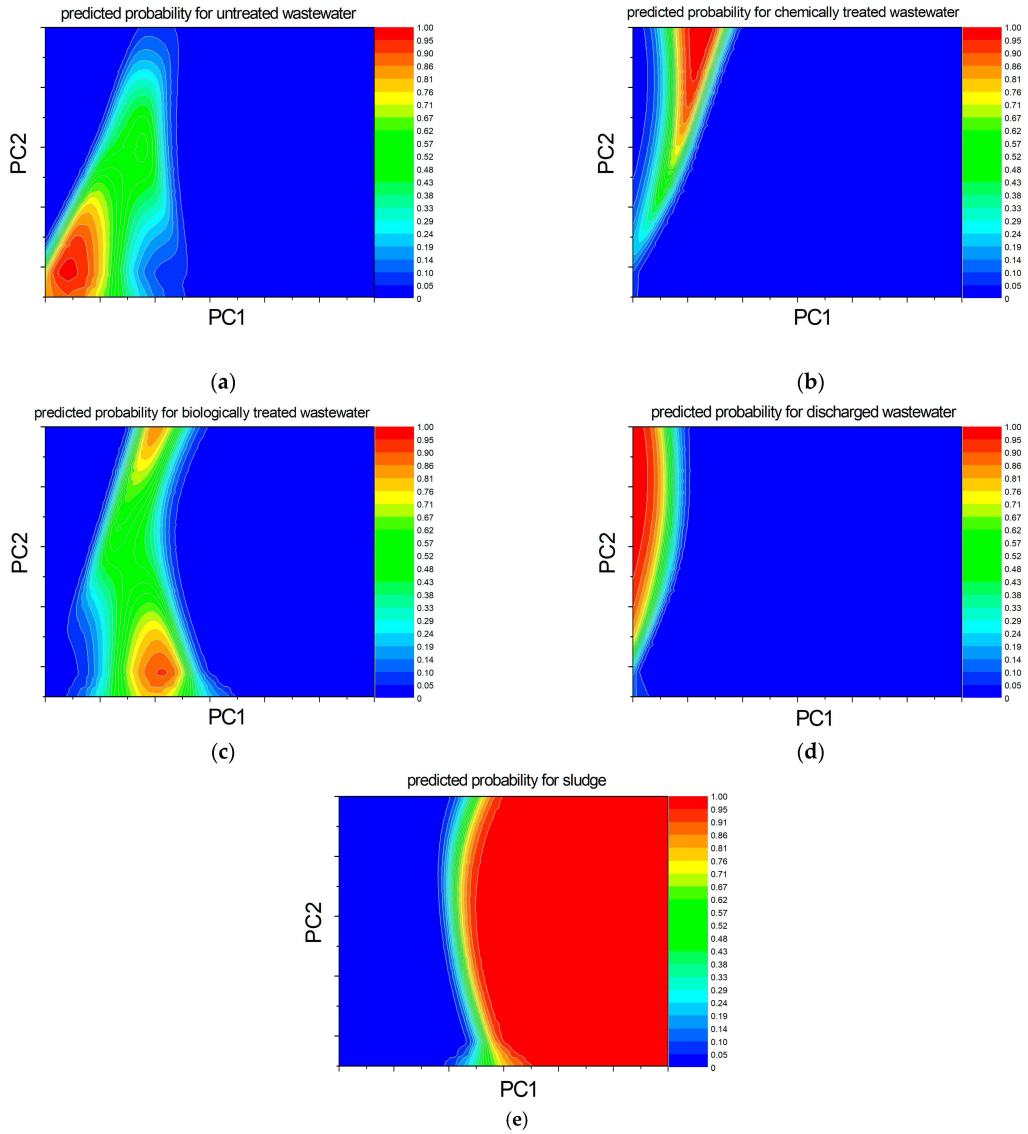

Figure 16. The predicted probability using ANN for (**a**) the untreated wastewater, (**b**) chemically treated wastewater (**c**) biologically treated wastewater (**d**) discharged wastewater and (**e**) sludge.

Such prediction maps were produced and discussed in [54], where Dragan et al. classify data measured by NMR and FT-IR to various types of colorectal cancer. However, according to our knowledge, this is the first time that such predictions are used to classify the wastewater and sludge resulted from slaughterhouse activity. Thus, one can say that this predictive approach validates the experimental data, which may be used an automated real-time monitoring along with an educated decision-making processes.

5. Conclusions

This is one of the most complex studies related to the characterization of wastewater collected from slaughterhouses. This complexity is based on both the large variety of measured parameters using modern and classical methods, and on the many levels of analysis which start with raw measurement, then continue with the ILT analysis of measured data and primary classification. This then continues with statistical analysis of principal components, which is finally used to train an artificial neural network to predict and classify new measurements. The advantage was demonstrated of using model-free low field ^{1}H NMR relaxometry and diffusometry combined with Laplace-like analysis compared to the classical methods, which provide a global single value for the entire sample, leading to a more realistic characterization of wastewater dynamic components. This analysis showed that the distributions of ^{1}H NMR transverse relaxation times T_2 present two distinct domains. The first characterizes water with dissolved solids and the second characterizes water with undissolved solids. Additionally, it was shown that the distribution of ^{1}H NMR self-diffusion coefficient D also presents two domains. These are self-diffusion in bulk water and the transported water attached to solid residues flowing by flotation and sedimentation. The ^{1}H NMR diffusometry measurements proved this, even though the discharged wastewater is not completely clean of undissolved solids. To assess the contribution of each parameter to the evaluation process of the efficiency of the purification treatment performed at a chicken slaughterhouse, a statistical analysis of principal components was performed. It was shown how the PCA analysis can be further improved if it is used to train an ANN to predict and classify a new measurement for one of the studied categories of wastewater or sludge. From the analysis of the distributions of transverse relaxation times T_2 and diffusion coefficient D, the VIS-nearIR spectra and EC and TDSS measured parameters, one can conclude that the purification process performed by the chicken slaughterhouse is efficient. Finally, this study demonstrates that, in addition to classical methods of analysis, which have their own merits but are limited to a single-value global characterization, the use of complementary methods, capable of emphasizing different components by providing a distribution of values for measured parameters and multi-level analysis, is an extraordinary tool that shows how each technique used for wastewater treatment works, what its advantages and disadvantages are, what its efficiency is, and what its limitations are and, above all, how it can be improved for a better treatment strategy. In particular, the proposed complex set of measurements of wastewater properties at every stage of the treatment process can provide useful information related to the complex interaction between treatment agent and wastewater components. Theis type of information can be used to design improved strategies for wastewater purification. The complex analysis (PCA combined with machine learning capable of prediction) can be used by industry to automate the monitoring process of wastewater treatment, but it is not limited to this. All these presented methods, experimental and numerical, are easily implemented in worldwide laboratories, since both low-field NMR and VIS-nearIR spectrometers have a relatively low acquisition and exploitation cost, therefore presenting a high probability of becoming a new standard in the field.

Supplementary Materials: The following are available online at https://www.mdpi.com/article/10.3390/w16172382/s1, Figure S1: The CPMG and PGSE pulse sequences; Figure S2: The T_2-distributions measured for sludge; Figure S3: The self-diffusion coefficient D distributions measured for sludge; Figure S4: The relationship between the total absorbance in the VIS-NearIR spectra and turbidity and Figure S5: The proportions and eigenvalues resulted from PCA applied on the measured parameters of poultry slaughterhouse wastewater.

Author Contributions: R.C. collected the samples, conceived, designed and performed the experiments, primary and secondary data analysis and statistical analysis, revised and proofread the paper; R.F. conceived and designed the experiments, wrote the numerical software for advanced data analysis, wrote and revised the paper. All authors have read and agreed to the published version of the manuscript.

Funding: This research received no external funding.

Data Availability Statement: The original contributions presented in the study are included in the article/Supplementary Materials, further inquiries can be directed to the corresponding author/s.

Acknowledgments: The authors would like to thank S.C. AGROPROD CRASNA Cooperativa Agricolă S.R.L., Satu-Mare, Romania, in particular Daniel Pereș and Petru Crainic. for providing the chicken slaughterhouse wastewater samples and relevant information about the wastewater treatment. The authors thank also Simona Nicoara for suggestions for English corrections.

Conflicts of Interest: The authors declare no conflicts of interest.

References

1. Paulista, L.O.; Presumido, P.H.; Peruço Theodoro, J.D.; Novaes Pinheiro, A.L. Efficiency analysis of the electrocoagulation and electroflotation treatment of poultry slaughterhouse wastewater using aluminum and graphite anodes. *Environ. Sci. Poll. Res.* **2018**, *25*, 19790–19800. [CrossRef]
2. Aceves-Lara, C.-A.; Latrille, E.; Conte, T.; Steye, J.-P. Online estimation of VFA, alkalinity and bicarbonateconcentrations by electrical conductivity measurementduring anaerobic fermentation. *Water Sci. Technol.* **2012**, *65*, 1281–1289. [CrossRef]
3. Yusoff, M.S.; Azwan, A.M.; Zamri, M.F.M.A.; Aziz, H.A. Removal of colour, turbidity, oil and grease for slaughterhouse wastewater using electrocoagulation method. *AIP Conf. Proc.* **2017**, *1892*, 040012.
4. Khanna, V.K. pH measurement of dirty water sources by ISFET: Addressing practical problems. *Sens. Rev.* **2007**, *27*, 233–238. [CrossRef]
5. Modla, M. The easy guide to pH measurement. *Meas. Control* **2004**, *37*, 204–206. [CrossRef]
6. Ferraz, F.M.; Yuan, Q. Nitrite interference with soluble COD measurements from aerobically treated wastewater. *Water Environ. Res.* **2017**, *89*, 549–554. [CrossRef]
7. APHA. *Standard Methods for the Examination of Water and Wastewater*, 22nd ed.; American Public Health Association: Washington, DC, USA, 2012.
8. Maremane, S.; Belle, G.; Oberholster, P. Assessment of Effluent Wastewater Quality and the Application of an Integrated Wastewater Resource Recovery Model: The Burgersfort Wastewater Resource Recovery Case Study. *Water* **2024**, *16*, 608. [CrossRef]
9. Alekseevsky, D.; Chernysh, Y.; Shtepa, V.; Chubur, V.; Stejskalová, L.; Balintova, M.; Fukui, M.; Roubík, H. Enhancing Ecological Efficiency in Biological Wastewater Treatment: A Case Study on Quality Control Information System. *Water* **2023**, *15*, 3744. [CrossRef]
10. El Aatik, A.; Navarro, J.M.; Martínez, R.; Vela, N. Estimation of Global Water Quality in Four Municipal Wastewater Treatment Plants over Time Based on Statistical Methods. *Water* **2023**, *15*, 1520. [CrossRef]
11. Mamun, M.; Kim, J.Y.; An, K.G. Multivariate Statistical Analysis of Water Quality and Trophic State in an Artificial Dam Reservoir. *Water* **2021**, *13*, 186. [CrossRef]
12. Boughou, N.; Majdy, I.; Cherkaoui, E.; Khamar, M.; Nounah, A. Physico-chemical characterization of wastewater from slaughterhouse: Case of rabat in Morocco. *ARPN J. Agric. Biol. Sci.* **2018**, *13*, 19–24.
13. Crainic, R.; Drăgan, L.R.; Fechete, R. ^{1}H NMR relaxometry and ATR-FT-IR spectrosopy used for the assesment of wastewater treatment in slaughterhouse. *Studia UBB Phys.* **2018**, *63*, 49–60. [CrossRef]
14. Seif, H.; Moursy, A. Treatment of slaughterhouse wastes. In Proceedings of the Sixth International Water Conference, IWTC, Alexandria, Egypt, 23–25 March 2001; pp. 270–271.
15. Alayu, E.; Yirgu, Z. Advanced technologies for the treatment of wastewaters from agro-processing industries and cogeneration of by-products: A case of slaughterhouse, dairy and beverage industries. *Int. J. Environ. Sci. Technol.* **2018**, *15*, 1581–1596. [CrossRef]
16. López-Maldonado, E.A.; Oropeza-Guzman, M.T.; Jurado-Baizaval, J.L.; Ochoa-Terán, A. Coagulation–flocculation mechanisms in wastewater treatment plants through zeta potential measurements. *J. Hazard. Mat.* **2014**, *279*, 1–10. [CrossRef]

17. Mehmood, K.; Rehman, S.K.U.; Wang, J.; Farooq, F.; Mahmood, Q.; Jadoon, A.M.; Javed, M.F.; Ahmad, I. Treatment of Pulp and Paper Industrial Effluent Using Physicochemical Process for Recycling. *Water* **2019**, *11*, 2393. [CrossRef]
18. Zamani, H.; Golestani, H.A.; Mousavi, S.M.; Zhiani, R.; Hosseini, M.S. Slaughterhouse wastewater treatment using biological anaerobic and coagulation-flocculation hybrid process. *Desal. Wat. Treat.* **2019**, *155*, 64–71. [CrossRef]
19. Lazaridis, N.K.; Matis, K.A.; Webb, M. Flotation of metal-loaded clayanion exchangers. Part I: The case of chromate. *Chemosphere* **2001**, *42*, 373–378. [CrossRef]
20. Doyle, F.M.; Liu, Z.D. The effect of triethylenetraamine (trien) on the ion flotation of Cu^{2+} and Ni^{2+}. *J. Colloid Interface Sci.* **2003**, *258*, 396–403. [CrossRef]
21. Khandegar, V.; Saroha, A.K. Electrocoagulation for the treatment of textile industry effluent e A review. *J. Environ. Manag.* **2013**, *128*, 949–963. [CrossRef]
22. Ozturk, D.; Yilmaz, A.E. Treatment of slaughterhouse wastewater with the electrochemical oxidation process: Role of operating parameters on treatment efficiency and energy consumption. *J. Water Proc. Eng.* **2019**, *31*, 100834. [CrossRef]
23. Tünay, O.; Kabdasli, N.I. Hydroxide precipitation of complexed metals. *Water Res.* **1994**, *28*, 2117–2124. [CrossRef]
24. Andrus, M.E. A review of metal precipitation chemicals for metal-finishing applications. *Metal Finish.* **2000**, *98*, 20–23. [CrossRef]
25. Chen, B.; Qu, R.; Shi, J.; Li, D.; Wei, Z.; Yang, X.; Wang, Z. Heavy metal and phosphorus removal from water by optimizing use of calcium hydroxide and risk assessment. *Environ. Pollut.* **2012**, *1*, 38–54. [CrossRef]
26. Yang, Z.; Zhou, Y.; Feng, Z.; Rui, X.; Zhang, T.; Zhang, Z. A Review on Reverse Osmosis and Nanofiltration Membranes for Water Purification. *Polymers* **2019**, *11*, 1252. [CrossRef] [PubMed]
27. Hacıfazlıoğlu, M.C.; Parlar, I.; Pek, T.Ö.; Kabay, N. Evaluation of chemical cleaning to control fouling on nanofiltration and reverse osmosis membranes after desalination of MBR effluent. *Desalination* **2019**, *466*, 44–51. [CrossRef]
28. Aziz, H.A.; Puat, N.N.A.; Alazaiza, M.Y.D.; Hung, Y.T. Poultry Slaughterhouse Wastewater Treatment Using Submerged Fibers in an Attached Growth Sequential Batch Reactor. *Int. J. Environ. Res. Public Health* **2018**, *15*, 1734. [CrossRef]
29. Pan, M.; Huang, X.; Wu, G.; Hu, Y.; Yang, Y.; Zhan, X. Performance of Denitrifying Phosphate Removal via Nitrite from Slaughterhouse Wastewater Treatment at Low Temperature. *Water* **2017**, *9*, 818. [CrossRef]
30. Álvarez-Méndez, S.J.; Ramos-Suárez, J.L.; Ritter, A.; González, J.M.; Pérez, Á.C. Anaerobic digestion of commercial PLA and PBAT biodegradable plastic bags: Potential biogas production and ^{1}H NMR and ATR-FTIR assessed biodegradation. *Heliyon* **2023**, *9*, e16691. [CrossRef]
31. Stapf, S.; Kimmich, R. Translational versus rotational molecular dynamics in plastic crystals studied by NMR relaxometry and diffusometry. *Mol. Phys.* **1997**, *92*, 1051–1060. [CrossRef]
32. Martini, F.; Carignani, E.; Nardelli, F.; Rossi, E.; Borsacchi, S.; Cettolin, M.; Susanna, A.; Geppi, M.; Calucci, L. Glassy and Polymer Dynamics of Elastomers by ^{1}H Field-Cycling NMR Relaxometry: Effects of Cross-Linking. *Macromolecules* **2020**, *53*, 10028–10039. [CrossRef]
33. Asano, A. Chapter One-NMR Relaxation Studies of Elastomers. In *Annual Reports on NMR Spectroscopy*; Academic Press: Cambridge, MA, USA, 2015; Volume 86, pp. 1–72. [CrossRef]
34. Wang, N.; Xia, Y. Anisotropic analysis of multi-component T_2 and $T_{1\rho}$ relaxations in achilles tendon by NMR spectroscopy and microscopic MRI. *J. Magn. Reson. Imaging* **2013**, *38*, 625–633. [CrossRef] [PubMed]
35. Navon, G.; Eliav, U.; Demco, D.E.; Blümich, B. Study of order and dynamic processes in tendon by NMR and MRI. *J. Magn. Reson. Imaging* **2007**, *25*, 362–380. [CrossRef] [PubMed]
36. Istrate, D.; Er Rafik, M.; Popescu, C.; Demco, D.E.; Tsarkova, L.; Wortmann, F.-J. Keratin made micro-tubes: The paradoxical thermal behavior of cortex and cuticle. *Int. J. Biol. Mac.* **2016**, *89*, 592–598. [CrossRef]
37. Demco, D.E.; Utiu, L.; Tillmann, W.; Blümich, B.; Popescu, C. Morphology and molecular dynamics of hard α-keratin under pressure by ^{1}H and ^{13}C solid-state NMR. *Chem. Phys. Lett.* **2011**, *509*, 62–66. [CrossRef]
38. Colicchio, I.; Demco, D.E.; Baias, M.; Keul, H.; Moeller, M. Influence of the silica content in SPEEK–silica membranes prepared from the sol–gel process of polyethoxysiloxane: Morphology proton mobility. *J. Membr. Sci.* **2009**, *337*, 125–135. [CrossRef]
39. Baias, M.; Demco, D.E.; Blümich, B.; Möller, M. State of water in hybrid sulfonated poly(ether ether ketone)–silica membranes by ^{1}H solid-state NMR. *Chem. Phys. Lett.* **2009**, *473*, 142–145. [CrossRef]
40. Lacan, I.; Moldovan, M.; Ardelean, I. The Influence of Chitosan on Water Absorption and Solubility of Calcium Phosphate Cement. *Coatings* **2023**, *13*, 1641. [CrossRef]
41. Toma, I.-O.; Stoian, G.; Rusu, M.-M.; Ardelean, I.; Cimpoeşu, N.; Alexa-Stratulat, S.-M. Analysis of Pore Structure in Cement Pastes with Micronized Natural Zeolite. *Materials* **2023**, *16*, 4500. [CrossRef]
42. Thomas, D.; Oros-Peusquens, A.-M.; Poot, D.; Shah, N.J. Whole-Brain Water Content Mapping Using Super-Resolution Reconstruction with MRI Acquisition in 3 Orthogonal Orientations. *Magn. Reson. Med.* **2022**, *88*, 2117–2130. [CrossRef]
43. Gussoni, M.; Greco, F.; Vezzoli, A.; Paleari, M.A.; Moretti, V.M.; Lanza, B.; Zetta, L. Osmotic and aging effects in caviar oocytes throughout water and lipid changes assessed by ^{1}H NMR T_1 and T_2 relaxation and MRI. *Magn. Reson. Imaging* **2007**, *25*, 117–128. [CrossRef]
44. Wu, B.; Zhou, K.; He, Y.; Chai, X.; Dai, X. Unraveling the water states of waste-activated sludge through transverse spin-spin relaxation time of low-field NMR. *Water Res.* **2019**, *155*, 266–274. [CrossRef] [PubMed]

45. Fechete, R.; Morar, I.A.; Moldovan, D.; Chelcea, R.I.; Crainic, R.; Nicoara, S.C. Fourier and Laplace-like low-field NMR spectroscopy: The perspectives of multivariate and artificial neural networks analyses. *J. Magn. Reson.* **2021**, *324*, 106915. [CrossRef] [PubMed]
46. Venkataramanan, L.; Song, Y.Q.; Hürlimann, M.D. Solving Fredholm integrals of the first kind with tensor product structure in 2 and 2.5 dimensions. *IEEE Trans. Sign. Proc.* **2002**, *50*, 1017–1026. [CrossRef]
47. Song, Y.Q.; Venkataramanan, L.; Hürlimann, M.D.; Flaum, M.; Frulla, P.; Straley, C. T_1–T_2 correlation spectra obtained using a fast two-dimensional Laplace inversion. *J. Magn. Reson.* **2002**, *154*, 261–268. [CrossRef]
48. Hürlimann, M.D.; Flaum, M.; Venkataramanan, L.; Flaum, C.; Freedman, R.; Hirasaki, G.J. Diffusion-relaxation distribution functions of sedimentary rocks in different saturation states. *Magn. Reson. Imaging* **2003**, *21*, 305–310. [CrossRef] [PubMed]
49. Fechete, R.; Demco, D.E.; Blümich, B. Parameter maps of ^{1}H residual dipolar couplings in tendon under mechanical load. *J. Magn. Reson.* **2003**, *165*, 9–17. [CrossRef]
50. Aursand, I.G.; Veliyulin, E.; Böcker, U.; Ofstad, R.; Rustad, T.; Erikson, U. Water and salt distribution in Atlantic salmon (Salmo salar) studied by low-field ^{1}H NMR, ^{1}H and ^{23}Na MRI and light microscopy: Effects of raw material quality and brine salting. *J. Agric. Food Chem.* **2008**, *57*, 46–54. [CrossRef]
51. Cheng, S.; Tang, Y.; Zhang, T.; Song, Y.; Wang, X.; Wang, H.; Wang, H.; Tan, M. Approach for monitoring the dynamic states of water in shrimp during drying process with LF-NMR and MRI. *Dry. Technol.* **2018**, *36*, 841–848. [CrossRef]
52. Carneiro, C.D.S.; Mársico, E.T.; Ribeiro, R.D.O.R.; Conte Júnior, C.A.; Álvares, T.S.; De Jesus, E.F.O. Quality attributes in shrimp treated with polyphosphate after thawing and cooking: A study using physicochemical analytical methods and Low-Field ^{1}H NMR. *J. Food Process. Eng.* **2013**, *36*, 492–499. [CrossRef]
53. Afifi, A.; May, S.; Clark, V.A. *Practical Multivariate Analysis*, 5th ed.; CRC Press: Boca Raton, FL, USA; Taylor and Francis Group: New York, NY, USA, 2012; pp. 357–379.
54. Dragan, L.R.; Andras, D.; Fechete, R. Fourier Transform Infrared (FT-IR) Spectroscopy and Proton Nuclear Magnetic Resonance (^{1}H NMR) Relaxometry and Diffusometry for the Identification of Colorectal Cancer in Blood Plasma. *Anal. Lett.* **2023**, *56*, 286–302. [CrossRef]
55. Shiffman, D. The Nature of Code. In *Simulating the Natural Systems with Processing*; No Starch Press: San Francisco, CA, USA, 2012.
56. Shiffman, D. The Nature of Code. In *Simulating the Natural Systems with Javascript*; No Starch Press: San Francisco, CA, USA, 2024.